

# Monte Carlo Methods for Accelerator Simulation and Photon Beam Modeling

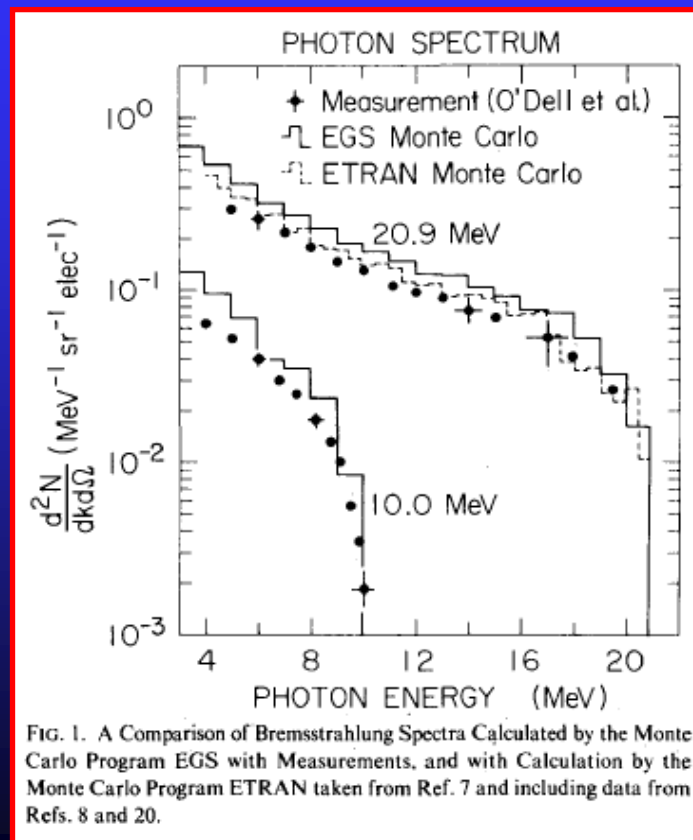
AAPM Summer School 2006  
Windsor, ON

Part I  
Daryoush Sheikh-Bagheri, PhD

Allegheny General Hospital  
Pittsburgh, PA

# A sample of work done ... 1

- McCall et al used MC simulations to study the effects of various targets and flattening filters on the mean energy of photon beams (McCall, McIntyre, and Turnbull 1978).



## A sample of work done ... 2

- Petti investigated the electron contamination in photon beams (Petti et al. 1983) by simulating a treatment machine head in great detail using a cylindrical geometry package to approximate various components of the linear accelerator.

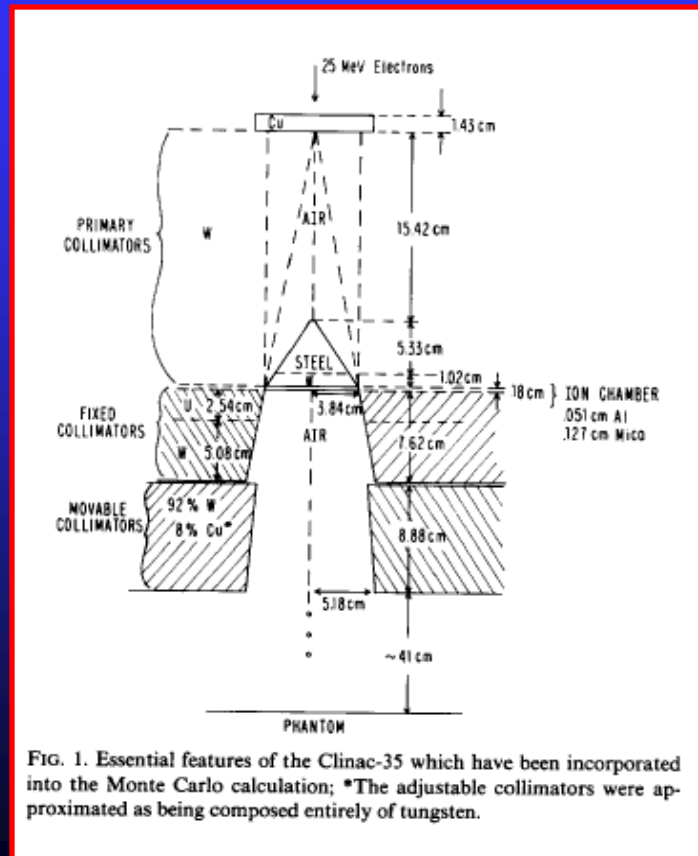


FIG. 1. Essential features of the Clinac-35 which have been incorporated into the Monte Carlo calculation; \*The adjustable collimators were approximated as being composed entirely of tungsten.

# A sample of work done ... 3

Mohan et al calculated photon spectra and fluence distributions from several accelerators (Mohan, Chui, and Lidofsky 1985).

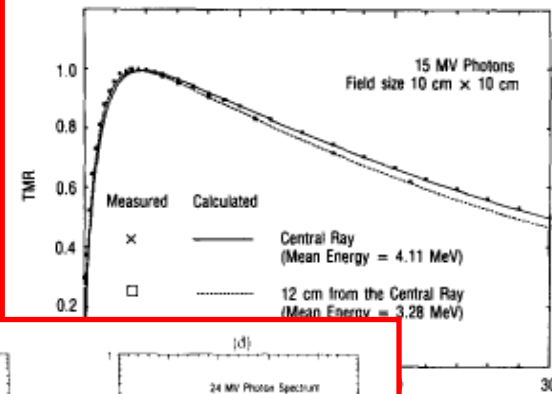
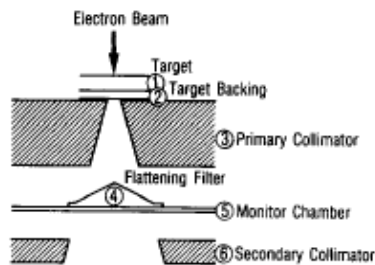


FIG. 2

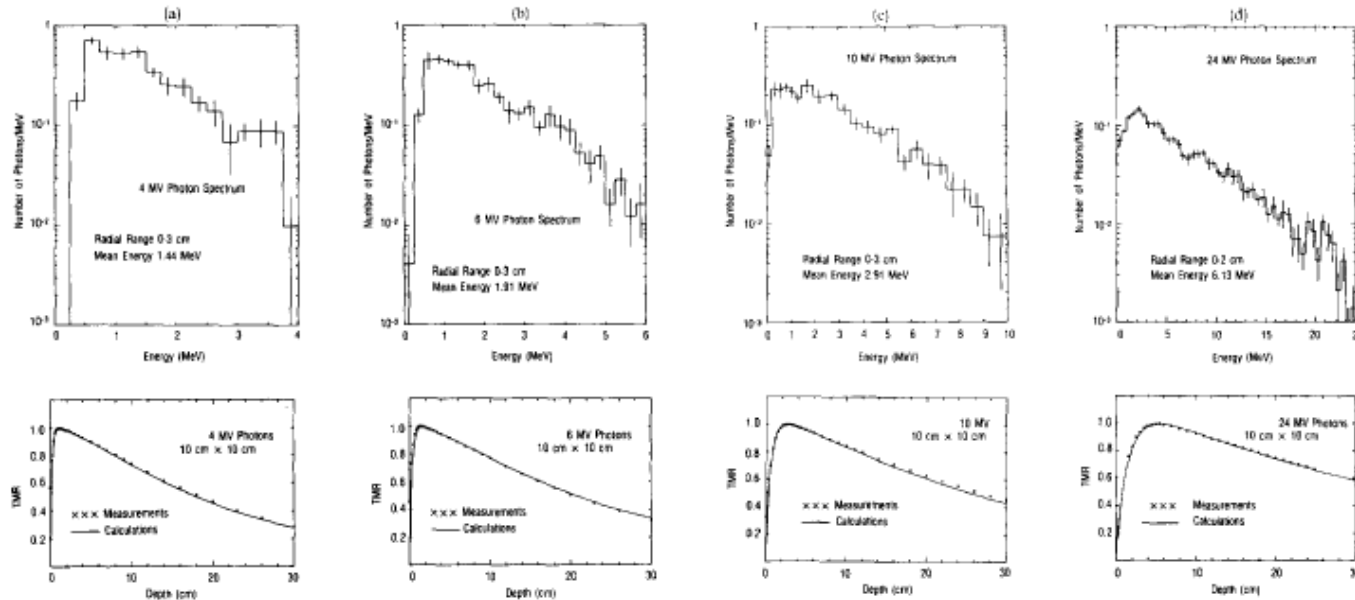


FIG. 7. Photon energy spectra and 10×10 cm TMR's for (a) Clinac-4 (4 MV), (b) Clinac-6 (6 MV), (c) Clinac-18 (10 MV), and (d) Clinac-2500 (24 MV).

## A sample of work done ... 4

Rogers et al (1988) investigated the sources of electron contamination in a  $^{60}\text{Co}$  beam.

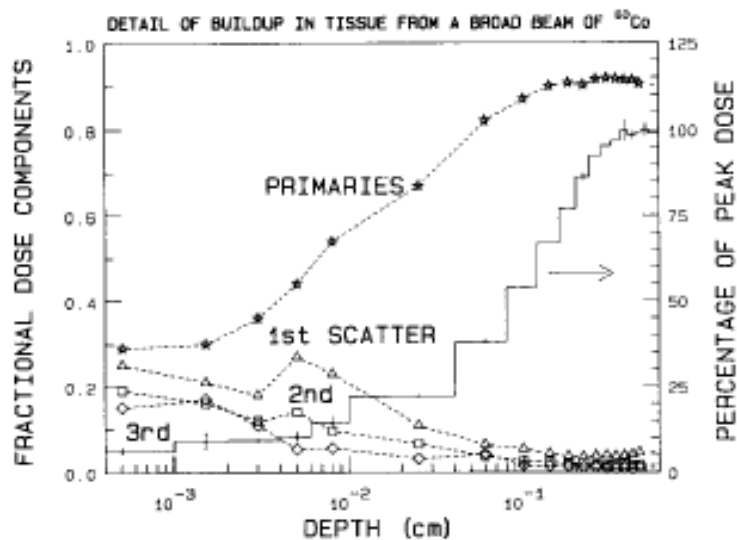


FIG. 4. Fractional dose components as a function of depth in the buildup region for a  $^{60}\text{Co}$  beam incident normally on a tissue phantom. The statistical uncertainties on the scatter components are quite large but the overall trends are clear. The corresponding depth-dose curve is also shown.

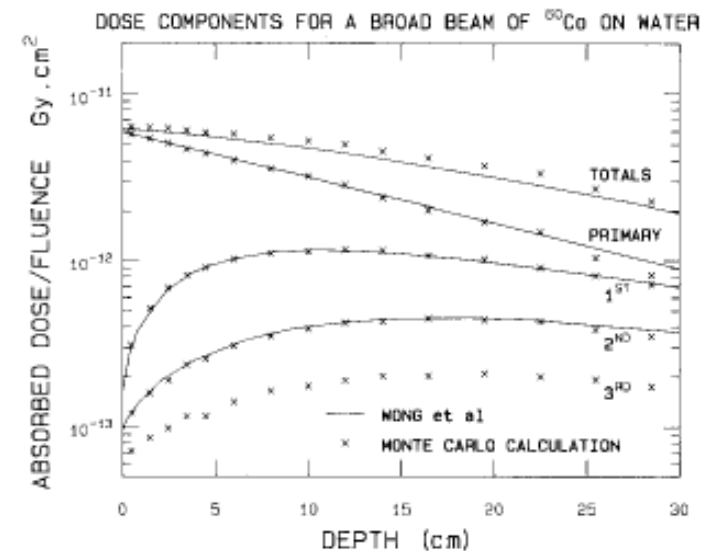


FIG. 6. Dose components as a function of depth throughout a 30-cm-thick water phantom for a normally incident broad parallel beam of  $^{60}\text{Co}$ . The solid lines are from analytic calculations by Wong *et al.* (Ref. 10), the  $\times$ 's are the current Monte Carlo calculations (which do not include electron transport in this case). The differences between the "totals" curves are an indication of the magnitude of third- and higher-order scatter contributions, which are only included in the Monte Carlo calculations.

# A sample of work done ... 5

Chaney et al simulated a 6MV photon accelerator to study the origins of head scatter (Chaney, Cullip, and Gabriel 1994).

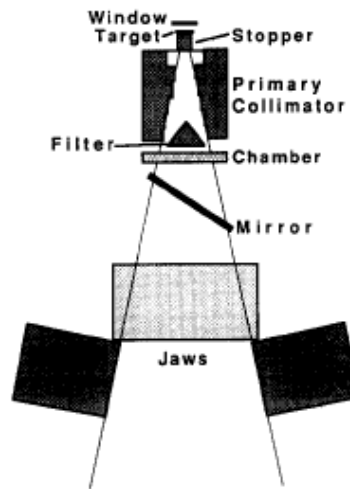


FIG. 1. Schematic drawing of the Siemens MD2 head modeled in this study.

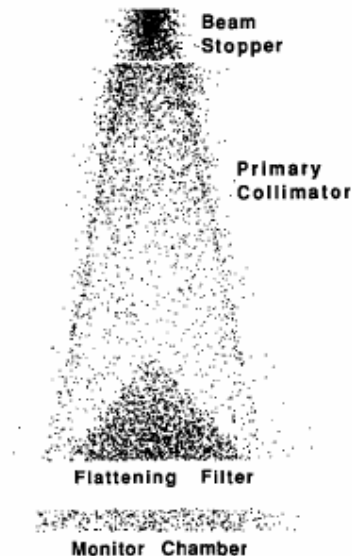


FIG. 7. Lateral view of the distribution of origin sites, represented as dots in space, for head scatter. Cloud formations of the beam stopper, primary collimator, flattening filter, and monitor chamber are clearly discernible.

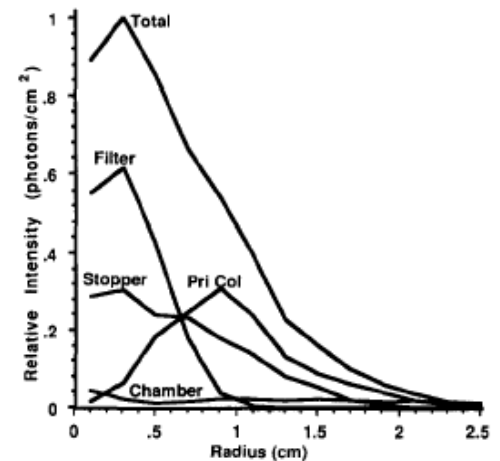


FIG. 8. Relative head scatter intensity distributions in a plane at the center of mass 6.2 cm from the target. The three-dimensional distribution was collapsed onto the plane by computing the intersection point for each scattered photon. The distributions for the flattening filter and primary collimator show dips near the CAX. For comparison, the maximum standard deviations for the composite and flattening filter curves are 0.04 and 0.02, respectively, at 0.1 cm.

## A sample of work done ... 6

- Lovelock et al (1994) simulated the photon beams from a Scanditronix MM50 machine to obtain the beam characteristics needed for treatment planning (Lovelock et al. 1994).

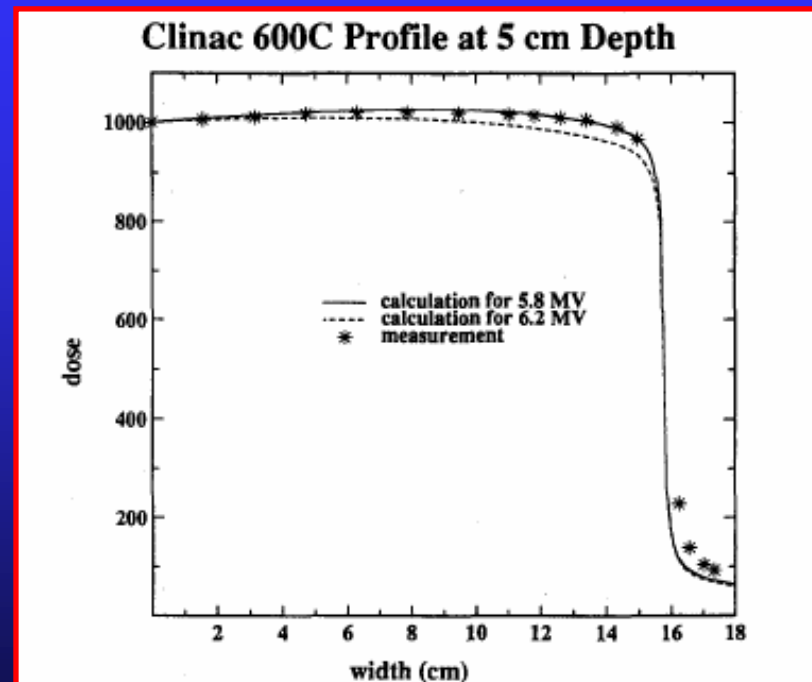
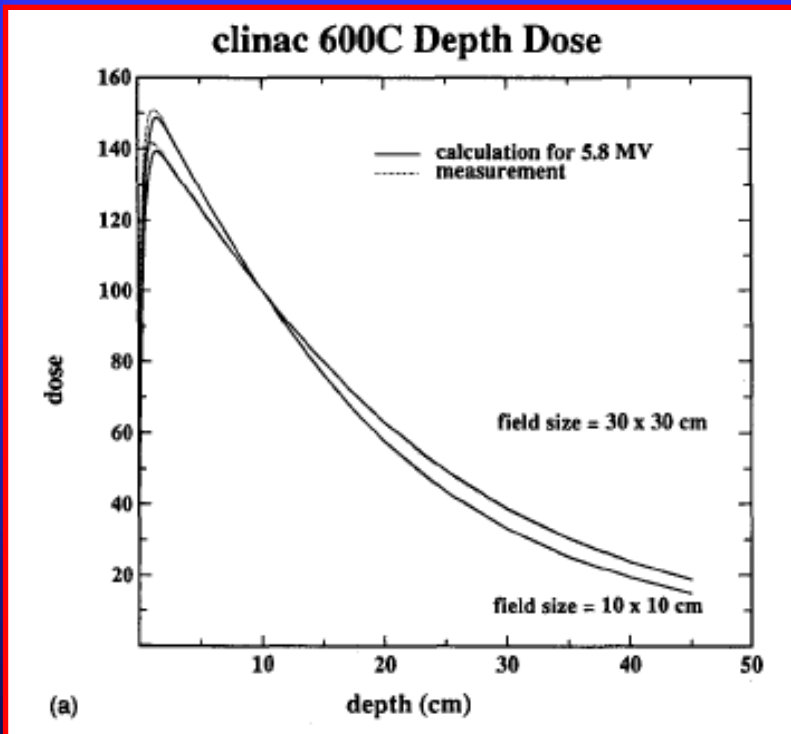


FIG. 2. The profiles for a 30×30 cm field at a depth of 5 cm calculated for the Clinac 600C beam using accelerating potentials of 5.8 and 6.2 MeV. The profiles at shallow depths are sensitive to small changes in the accelerating potential. The measured curve is shown for comparison.

# A sample of work done ... 7

- Sixel and Faddegon simulated a Therac-6 treatment head in radiosurgery mode using a cylindrically symmetric geometry (Sixel and Faddegon 1995).

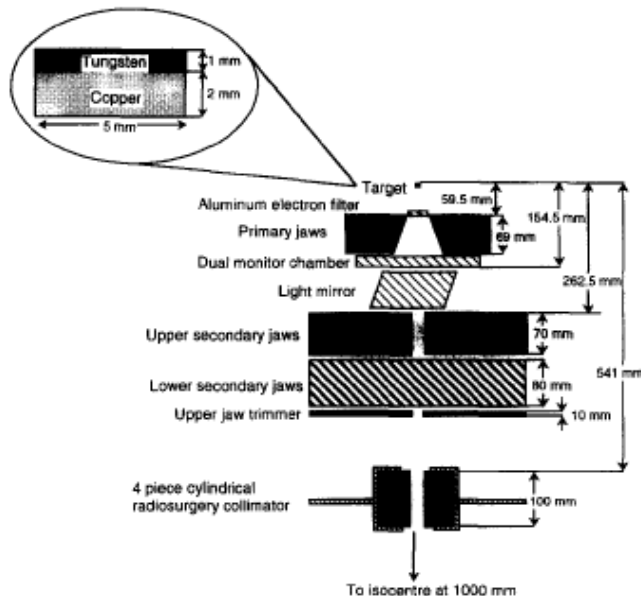


FIG. 1. Schematic diagram of Therac-6 linac head in radiosurgery mode. The sketch traces photons from the target through the aluminum electron filter and the beam collimation system. The insert shows the dimensions and composition of the target.

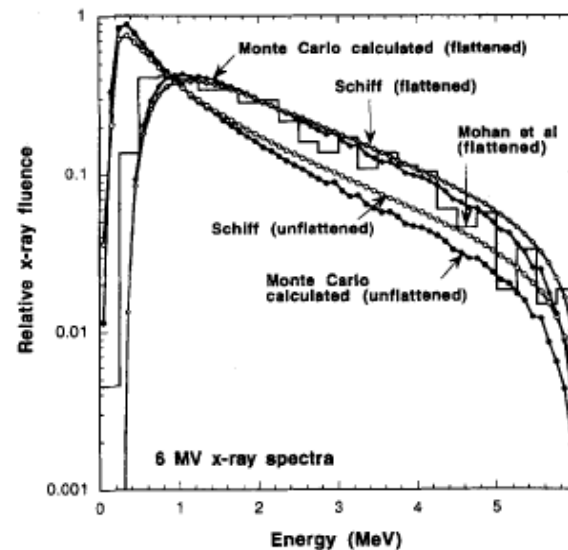
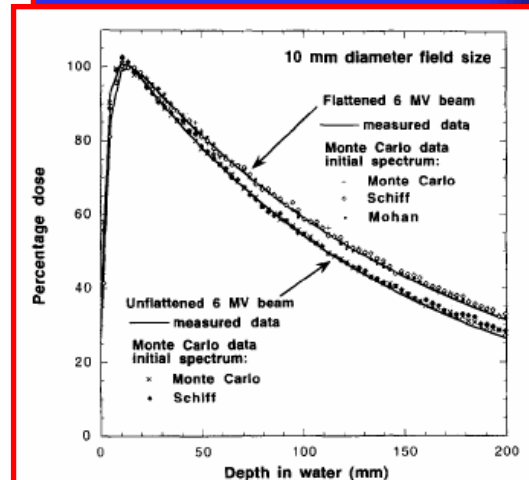


FIG. 2. Flattened and unflattened 6 MV radiosurgical x-ray spectra. Relative x-ray fluence is plotted as a function of energy. Shown are the Monte Carlo calculated unflattened (solid circles), the Schiff unflattened (open circles), the Monte Carlo calculated flattened (solid diamonds), and the Schiff flattened (open diamonds) spectra. The flattened fluence is calculated by attenuating the unflattened beams through the lead flattening filter. The Mohan *et al.* spectrum (solid line) is also plotted. The radial range of the Monte Carlo calculated spectra is 0–5 cm at 100 cm SSD.





## A sample of work done ... 8

- To study the differential beam hardening effect of the flattening filter, Lee simulated the 6 MV beam from a Varian Clinac 2100C accelerator using the EGS4 code (Lee 1997).

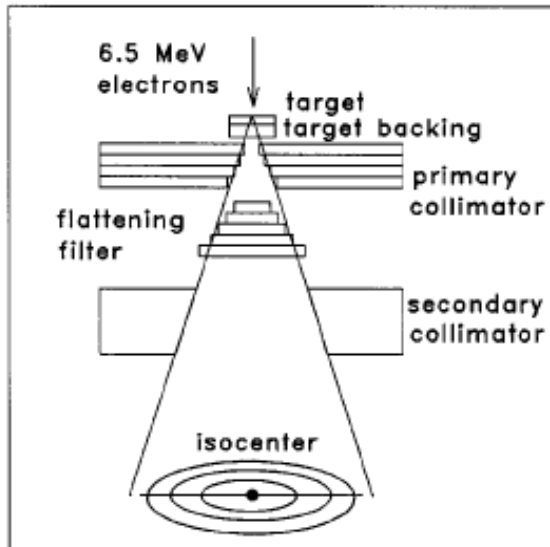


FIG. 1. A schematic diagram showing the major components of the simulation geometry.

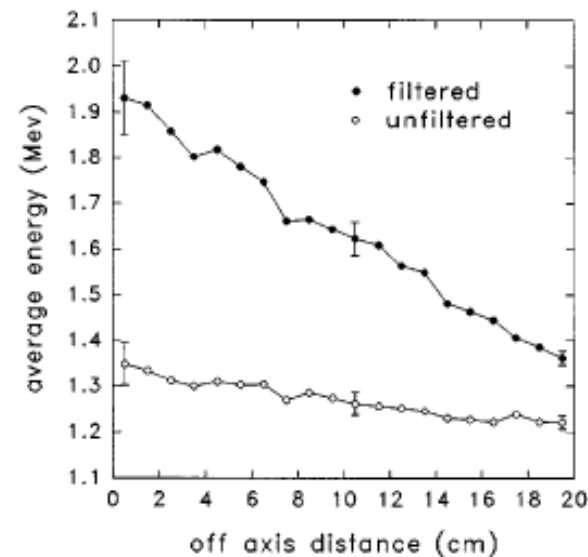


FIG. 3. Fluence-weighted photon energy of the filtered and unfiltered 6-MV beams as a function of the OAD. Closed circles: filtered beam; open circles: unfiltered beam. Error bars are also indicated.

# A sample of work done ... 9

- To determine the parameters in their photon source model used for dose calculation in the PEREGRINE system, Hartmann-Siantar et al simulated linacs using MCNP and the EGS4/BEAM code (Hartmann-Siantar 1997 & 2001).

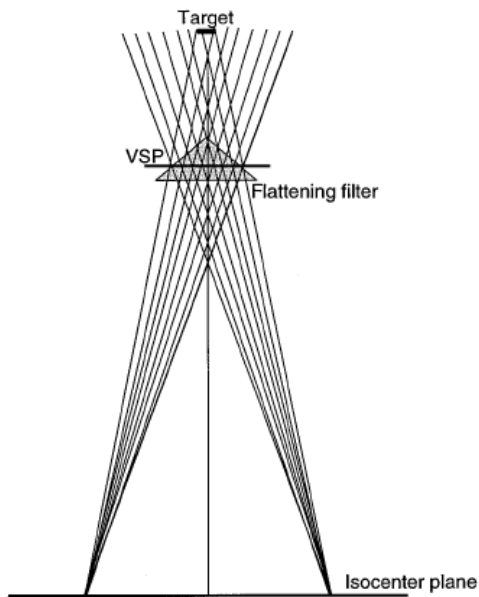


FIG. 1. The trajectories of particles that scatter from the flattening filter and cross the isocenter plane in a given tile form an hourglass figure with a neck close to the flattening filter.

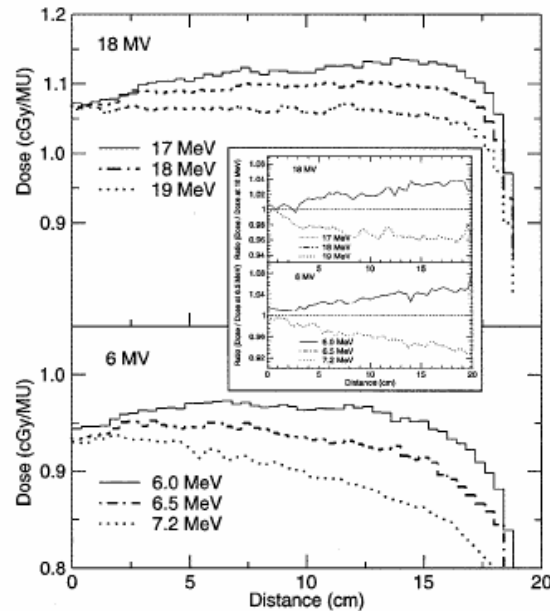


FIG. 6. Profiles at 10 cm depth for a  $38 \times 38 \text{ cm}^2$  field incident on a water phantom at 90 cm SSD, showing the effect of varying the initial electron energy. The largest-field profile is most sensitive to initial electron energy. Profiles at 10 cm depth were chosen because of their insensitivity to the effects of contamination electrons. The inset shows ratios of the profiles with respect to the profile for the 18 and 6.5 MV profiles, respectively.

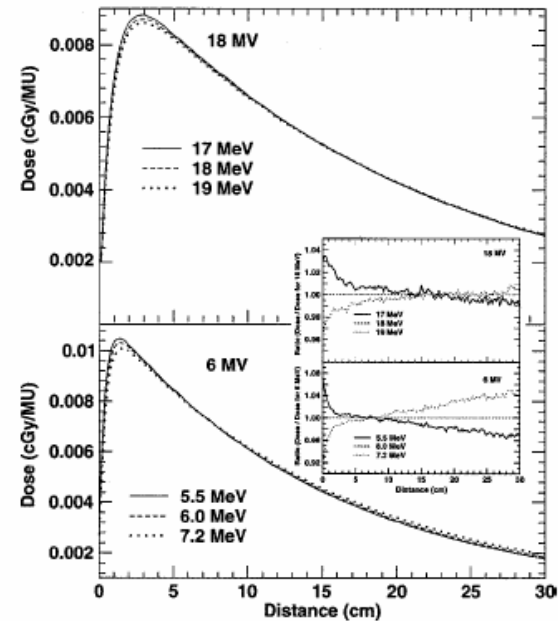


FIG. 7. Central-axis depth-dose curves for a  $2 \times 2 \text{ cm}^2$  field incident on a water phantom at 90 cm SSD, showing the effect of varying the initial electron energy. The  $2 \times 2 \text{ cm}^2$  field has the depth-dose curve that is the most sensitive to initial electron energy. The inset shows ratios of the profiles with respect to the profile for the 18 and 6.0 MV profiles, respectively.

# A sample of work done ... 10

- DeMarco et al simulated photon beams from Philips SL-15/25 linear accelerators to obtain the phase space information for patient dose calculation (DeMarco, Solberg, and Smathers 1998).

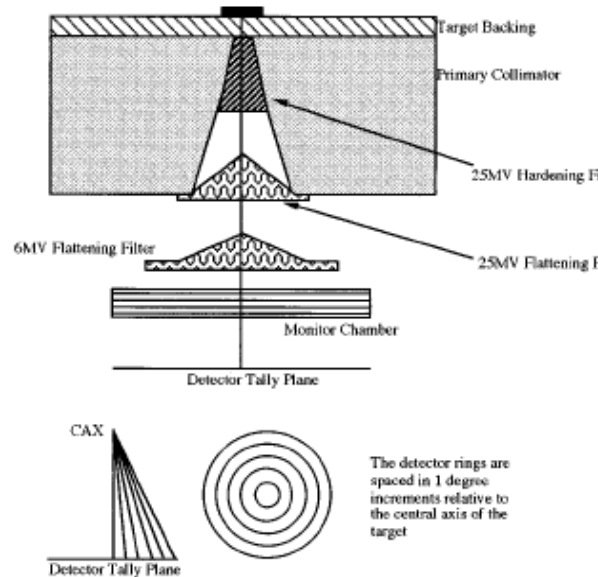


FIG. 4. MCNP4A simulation geometry for the linear accelerator treatment head. The detector tally plane is located 25 cm downstream from the front surface of the target. The circular rings correspond to the setup location for the MCNP4A ring detectors spaced in  $1^\circ$  increments relative to the beam central axis.

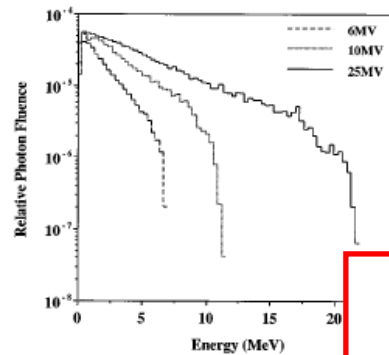
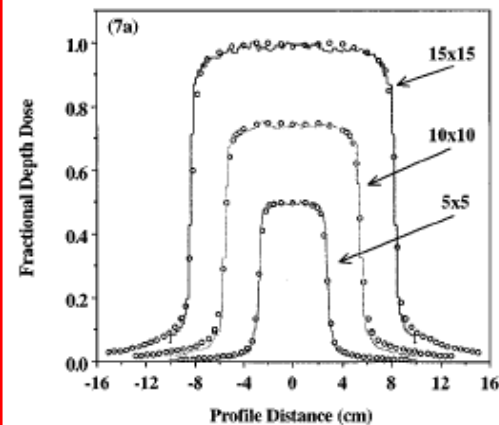
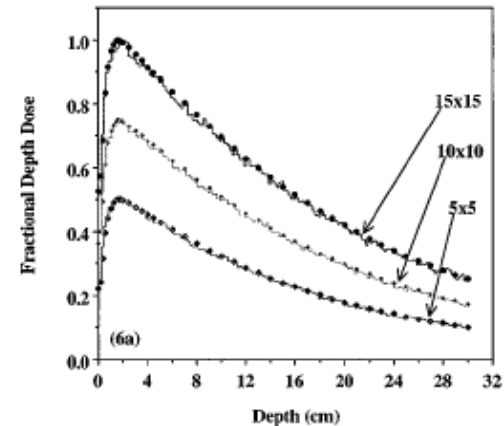


FIG. 5. The calculated bremsstrahlung spectra for the Philips SL-15/25 MV photon beam energies. The next-event-estimator tally was placed 25 cm downstream from the front surface of the target along the central axis. The three beam mean energies correspond to a mean electron energy of 6.8, 10.4, and 22.0 MeV for the 6, 10, and 25 MV photon beams, respectively.



## AS

- A more detailed re...
- the EGS4/BEAM cod...
- Some of the results...

### Comparison of measure... from the NRC linac

Daryoush Sheikh-Bagheri<sup>a)</sup>  
*Ionizing Radiation Standards, In...*  
*National Research Council Cana...*  
*and Ottawa Carleton Institute of*

D. W. O. Rogers,<sup>b)</sup> Carl K.  
*Ionizing Radiation Standards, In...*  
*National Research Council Cana...*

(Received 30 March 2000; ac...

### Sensitivity of megavo... to electron beam and

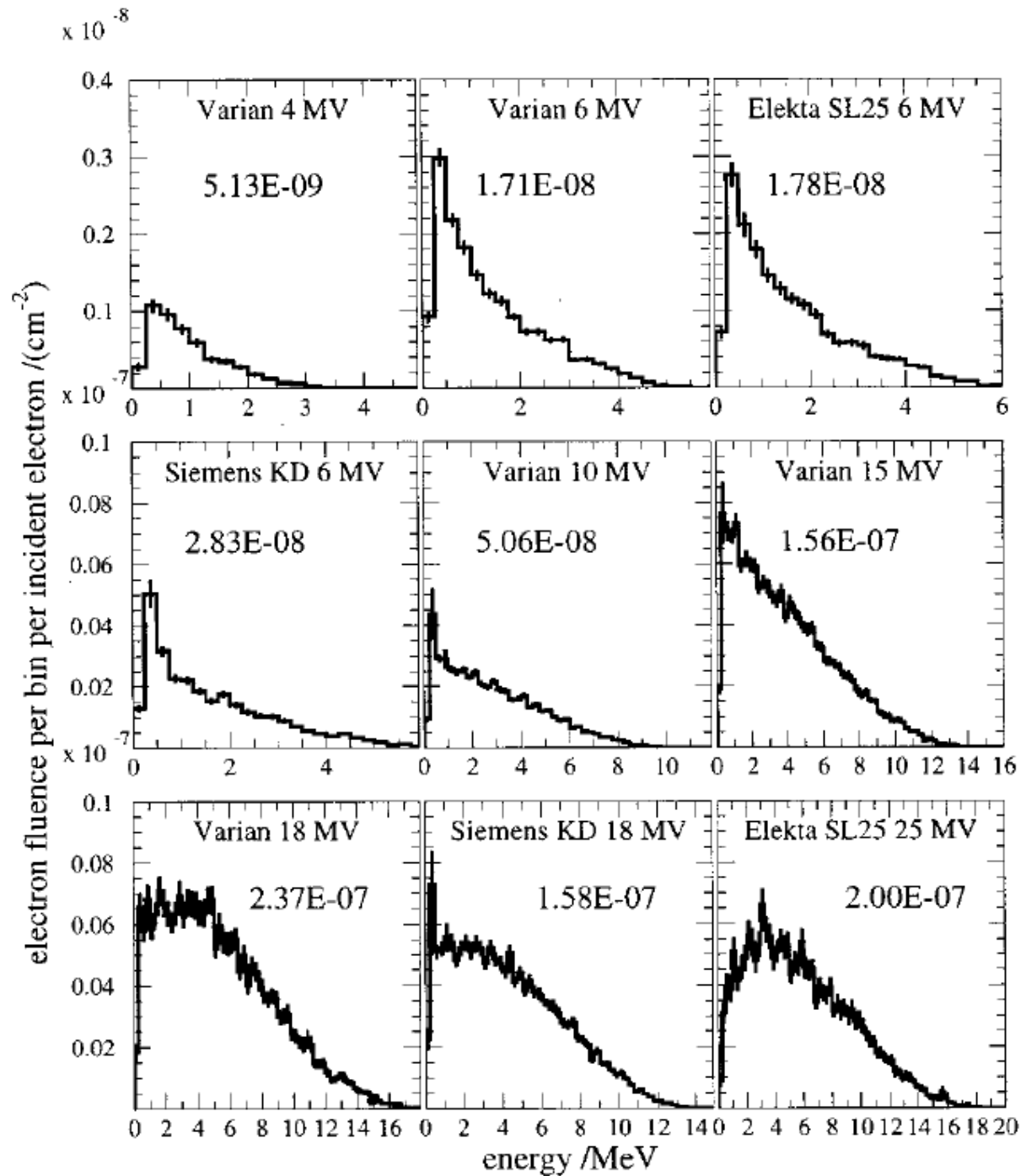
Daryoush Sheikh-Bagheri  
*Ionizing Radiation Standards,*

(Received 21 May 2001; ac...

### Monte Carlo calculati... using the BEAM code

Daryoush Sheikh-Bagheri  
*Ionizing Radiation Standards,*

(Received 10 August 2001...



## A sample of work done ... 12

- Another MC system, PENELOPE, was also used to simulate photon beams from a Saturne 43 accelerator (Mazurier et al. 1999).
- Balog et al simulated the multileaf collimator (MLC) interleaf transmission by simulating the NOMOS MIMiC MLC attached to a GE Orion 4 MV linear accelerator (Balog et al. 1999).
- The treatment head of a Siemens MXE accelerator was simulated to design a new flattening filter for the 6 MV photon beam for this machine (Faddegon, O'Brien, and Mason 1999).
- Verhaegen et al applied the EGS4/BEAM code to the simulation of radiotherapy kV x-ray units (Verhaegen et al. 1999).
- Detailed reviews on MC simulation and modeling of clinical photon and electron beams for radiation therapy (Ma and Jiang 1999) and (Verhaegen and Seuntjens 2003).

# Accelerator Simulation

- Several general-purpose MC code systems have been used for radiotherapy beam modeling including ETRAN/ITS, EGS4, EGSnrc, MCNP4/MCNP5, PENELOPE, GEANT3/ GEANT4. (see Verhaegen and Seuntjens 2003).
- Allow building an accelerator from a series of components
- Allow for tagging particles based on the interactions they undergo and location of the interactions

# Simulation Accuracy

- A goal of 2%/2 mm practical and adequate (Chetty et al., 2006)
- Agreement better than 1% could be achieved by fine-tuning
- Probably overkill (since 2-3% dosimetric uncertainty in machine commissioning)
- Overall accuracy of 5%/5 mm feasible, if relative doses to 3%/3 mm and calibration dose to 2%/2 mm (Faddegon et al. 1998)

# Simulation Efficiency

- Typically,  $10^8 - 10^9$  photons are needed for treatment planning dose calculation
- The total CPU time required to simulate all the photon and electron energies clinically used will be days using a state of the art desktop computer
- Iterative process of fine-tuning electron incident energy and other accelerator parameters for all the beams
- The real leap has been made possible by the use of various variance reduction techniques



# Simulation Geometry

- All the required materials and geometric data to build the MC simulation geometry:
  - have to be obtained either from the linac manufacturer(s)or
  - measured directly
- Note:
  - accelerator repairs, improvements or updates
  - same model may not have the same exact components
  - different scattering foils, flattening filters, monitor chambers or applicators.

# Phase Space Information

## phase space

*noun*

*(physics) an ideal space in which the coordinate dimensions represent the variables that are required to describe a system or substance*

*- WordReference.com*

- Standardized format recommended by IAEA consultant group (Capote et al. 2006).

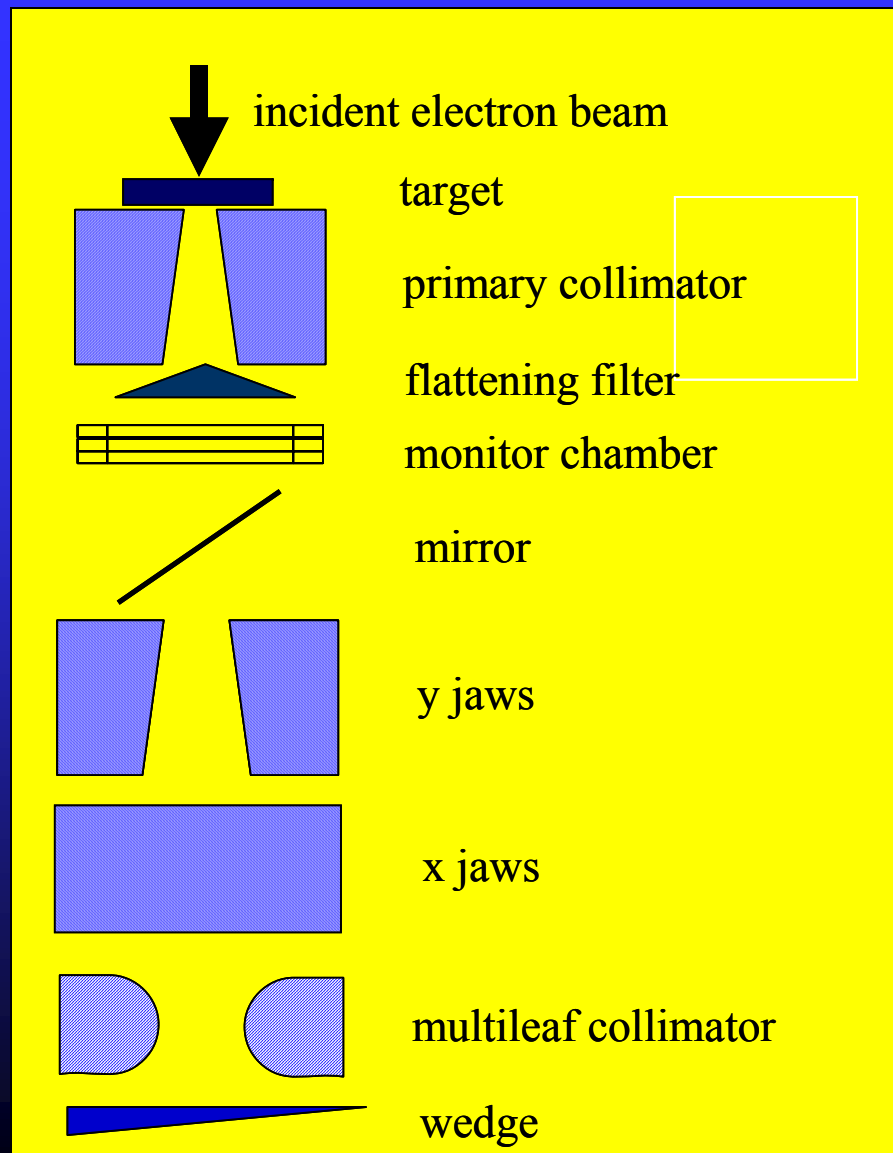




# IAEA recommended phase space variables (Capote et al. 2006).

Variable	Meaning	Type of variable returned
X	Position in X direction in cm	Real*4
Y	Position in Y direction in cm	Real*4
Z	Position in Z direction in cm	Real*4
U	Direction cosine along X	Real*4
V	Direction cosine along Y	Real*4
E	Kinetic energy in MeV	Real*4
Statistical_weight	Particle statistical weight	Real*4
Particle_type	Type of the particle	Integer*2
Sign_of_W	Sign of W (direction cosine in Z)	Logical*1
Is_new_history	Signifies if particle belongs to new history	Logical*1
Integer_extra	Extra storage space for variables (e.g., EGS LATCH, incremental history number, PENELOPE ILB, etc.)	$n*(Integer*4)$ ( $n \geq 0$ )
Float_extra	Extra storage space for variables (e.g., EGS ZLAST)	$m*(Real*4)$ ( $m \geq 0$ ) AGH

# Typical components of a MC model of a medical linac



# "Reference" Phase Space Files

**Reference photon dosimetry data and reference phase space data for the 6 MV photon beam from Varian Clinac 2100 series linear accelerators**

Sang Hyun Cho,<sup>a)</sup> Oleg N. Vassiliev, Seungsoo Lee, H. Helen Liu, Geoffrey S. Ibbott, and Radhe Mohan

*Department of Radiation Physics, The University of Texas M. D. Anderson Cancer Center, 1515 Holcombe Boulevard, Unit 547, Houston, Texas 77030*

(Received 5 January 2004; revised 15 October 2004; accepted for publication 15 October 2004; published 20 December 2004)

RPSDs available on the RPC website (<http://rpc.mdanderson.org>)



How accurate would a Monte Carlo  
simulation of photon beams  
turn out to be ...

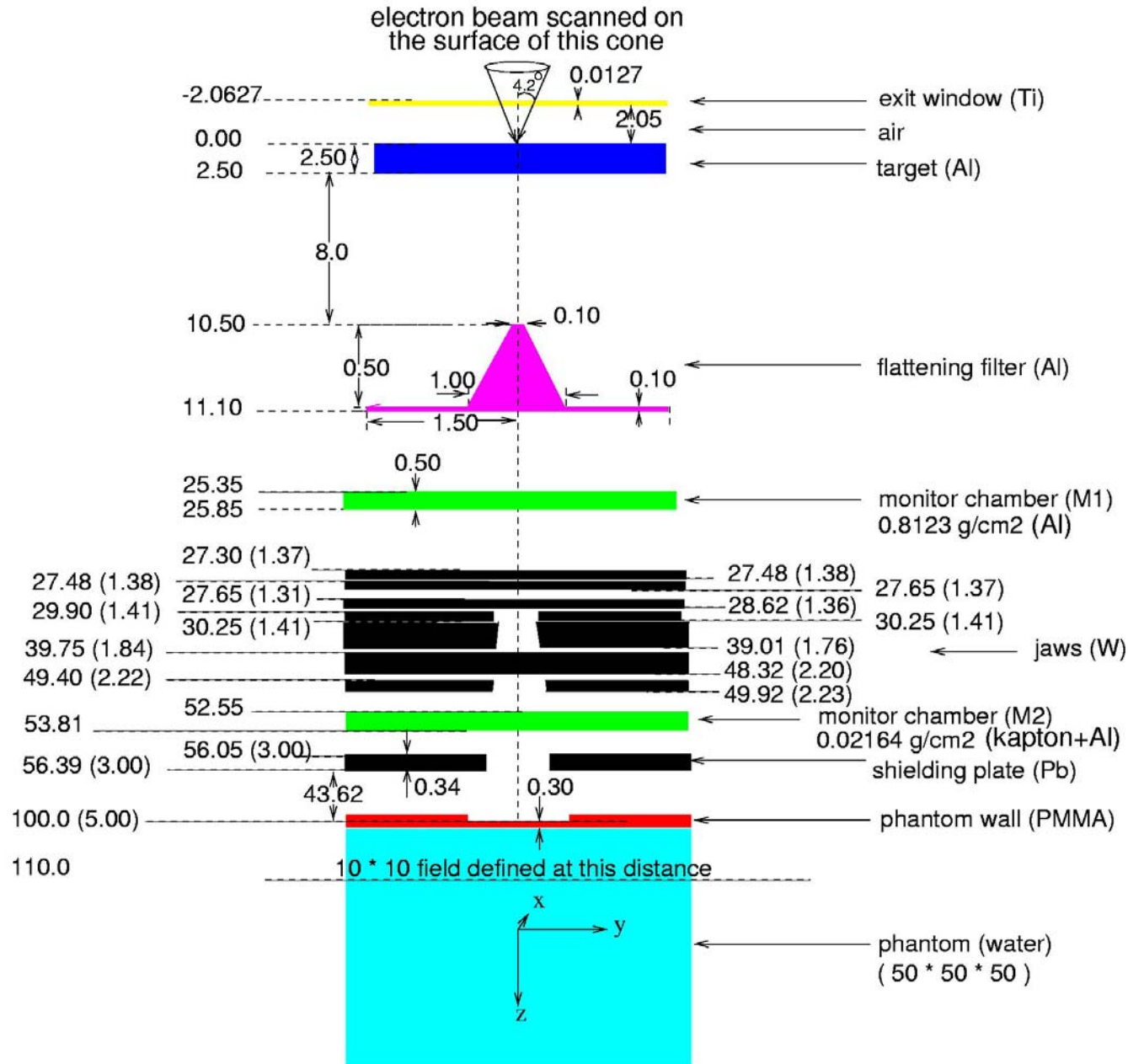
if we had "all" the information that  
we typically need to model a linac?

Lessons learned from BEAM code  
photon beam benchmark study ...

... a while ago ...



# NRCC, 10 MV photon beam

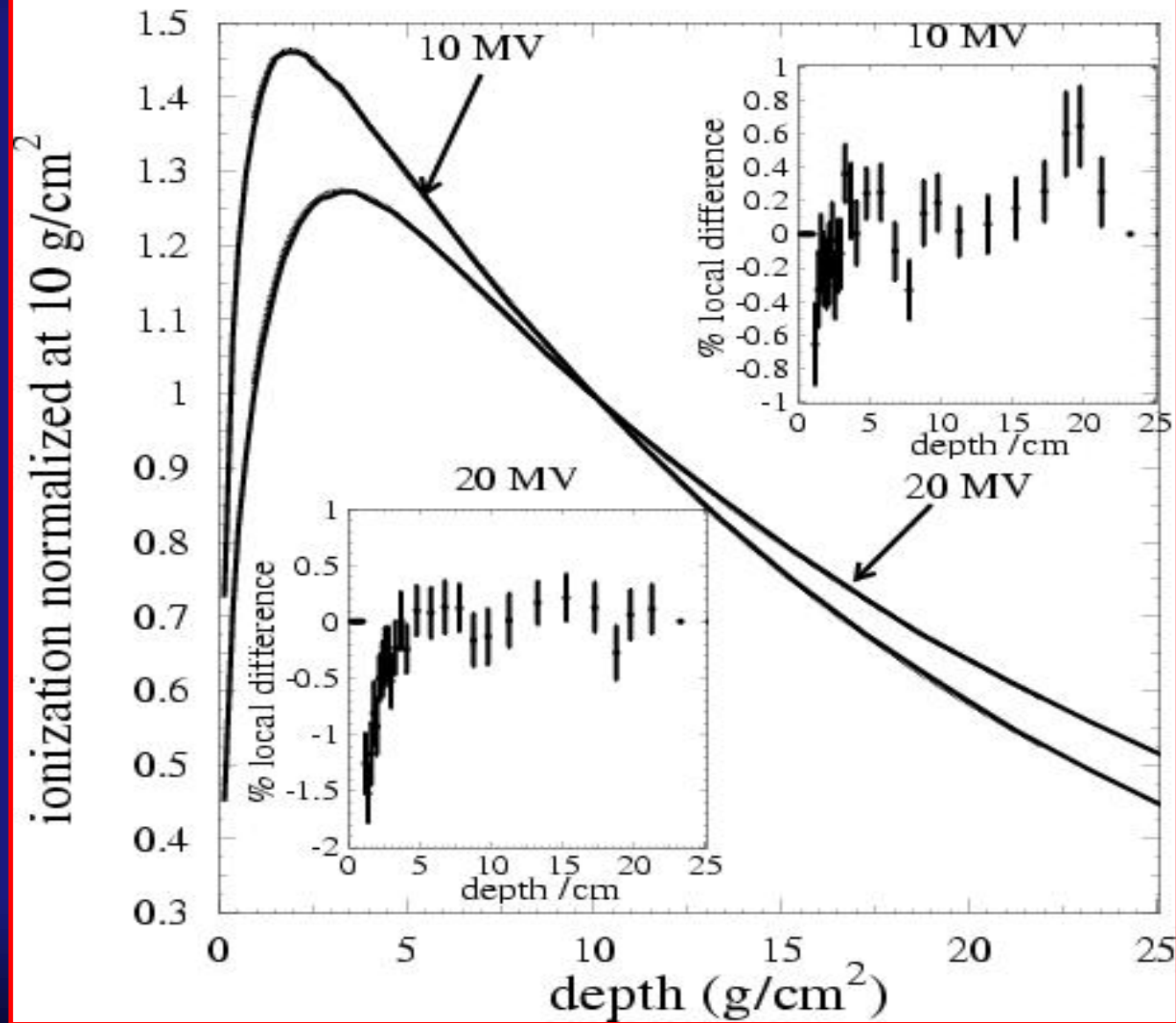


Med Phys  
27(10):  
2256-2266

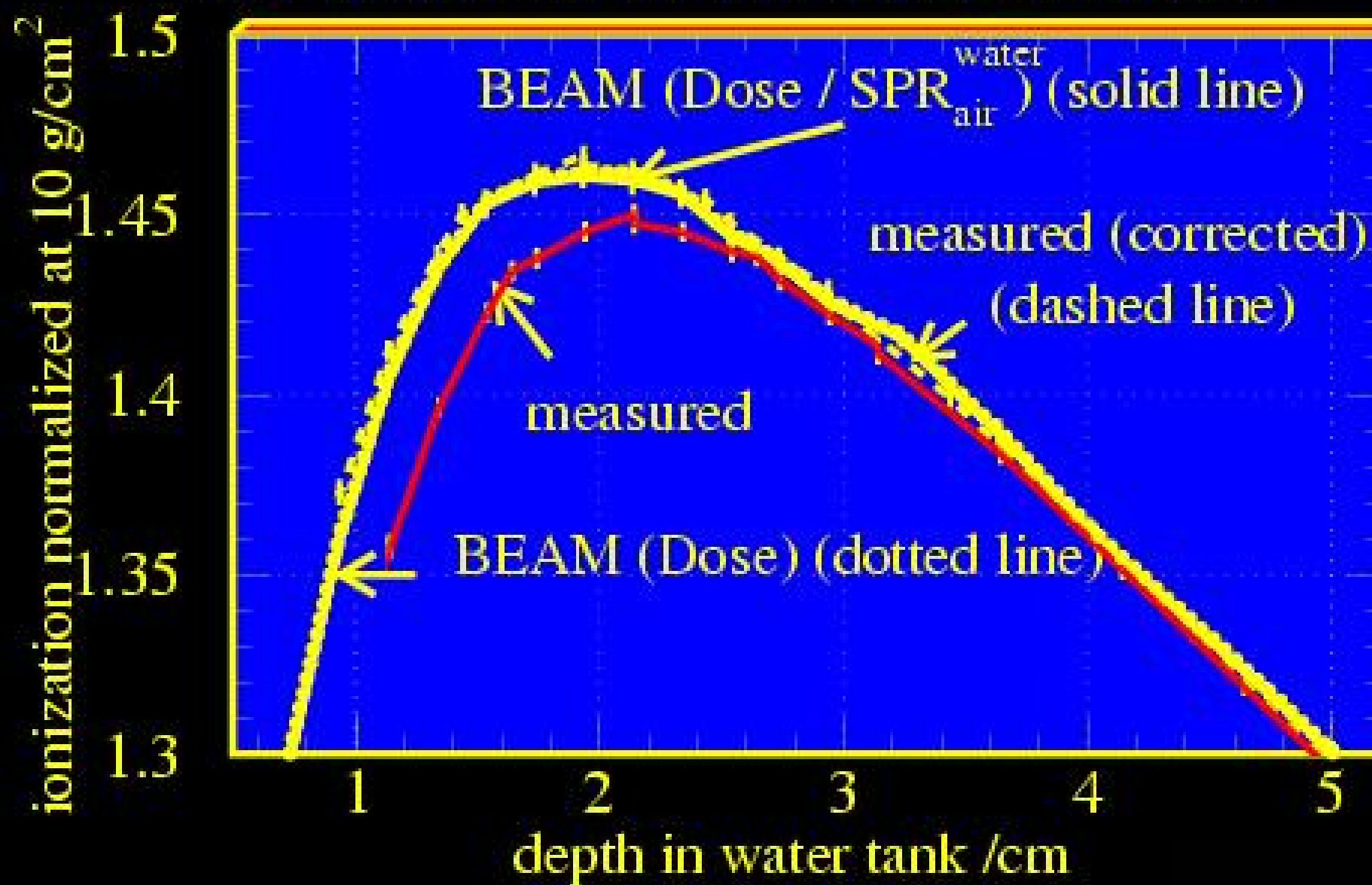




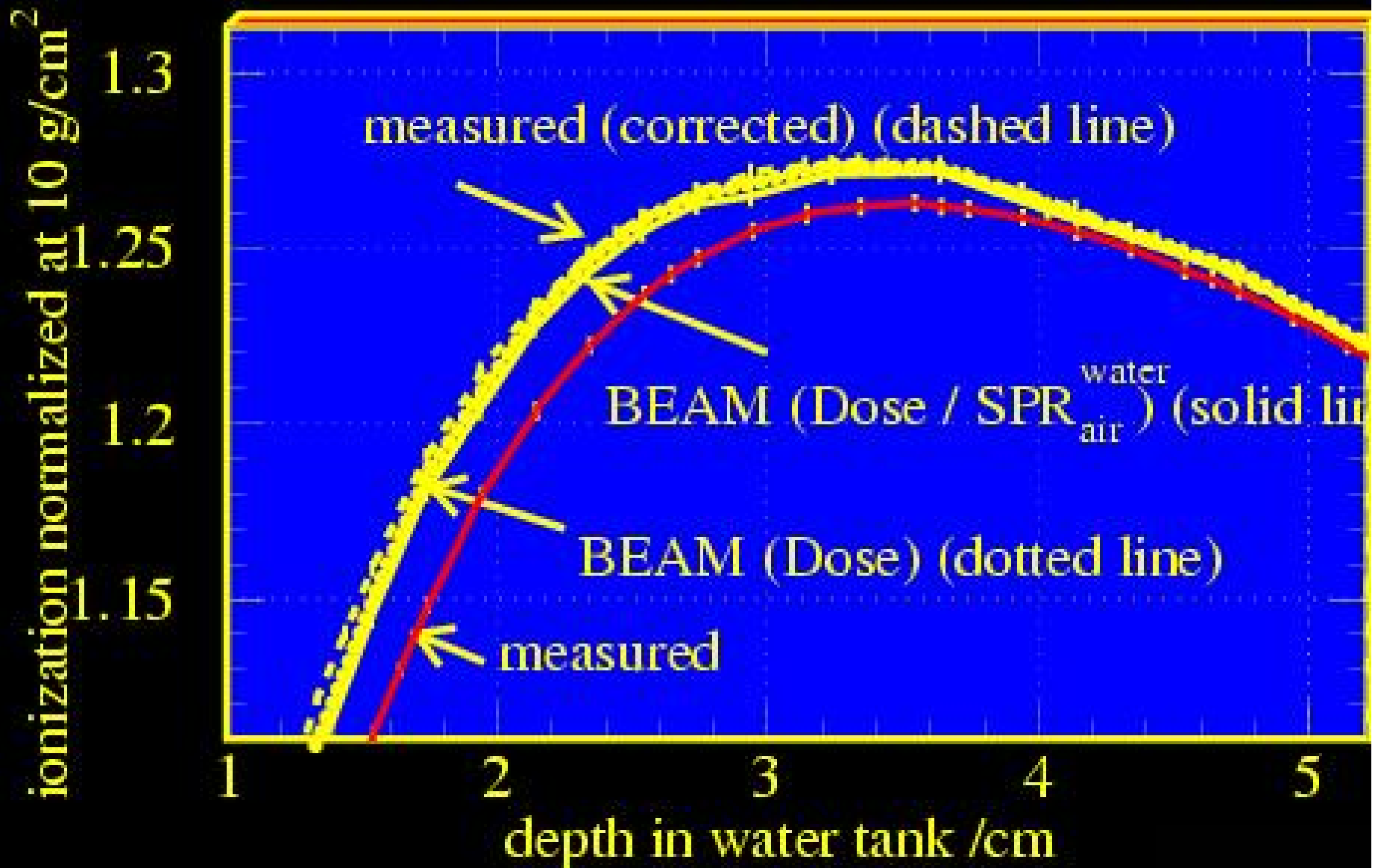
nic10\_x2\_xyz\_f60, 10MV energy fluence at z=10 cm



# 10 MV beam central-axis %dd in the build-up region

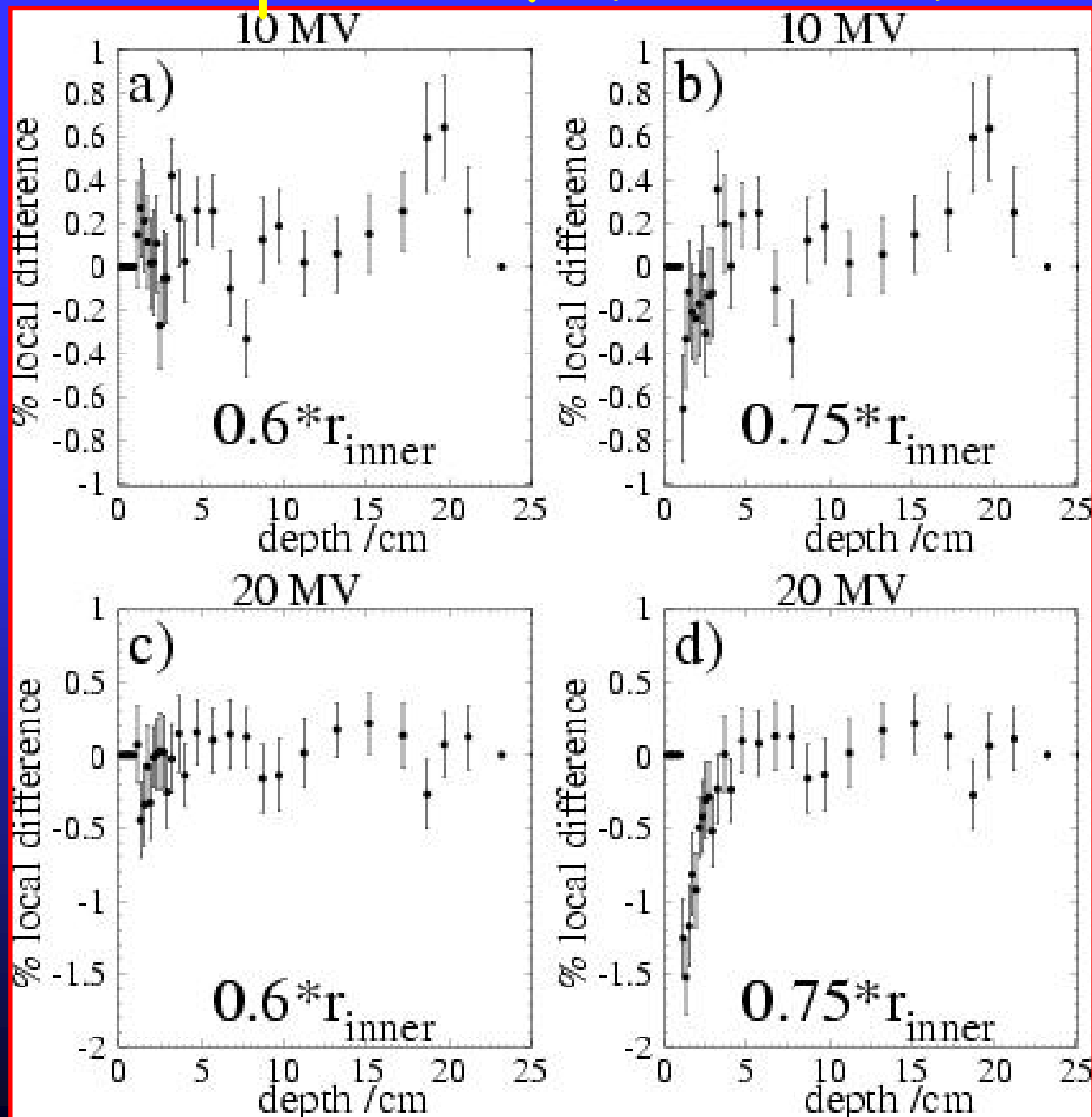


# 20 MV beam central-axis %dd in the build-up region



# The effective point of measurement

Med Phys  
27(10):  
2256-2266



# More Recent Studies of Build-up Dose

## On the effective point of measurement in megavoltage photon beams

Iwan Kawrakow

*Ionizing Radiation Standards, NRC, Ottawa, K1A 0R6*

(Received 6 October 2005; revised 24 January 2006; accepted for publication 6 April 2006;  
published 25 May 2006)

### Listed:

- Cross section inaccuracies (radiative corrections)

### Investigated in detail:

- The effective point of measurement (EPOM)
- EPOM shift is dependent on every detail of the ionization chamber (cavity length and radius, wall material density and thickness, central electrode radius) in addition to the beam energy and field size

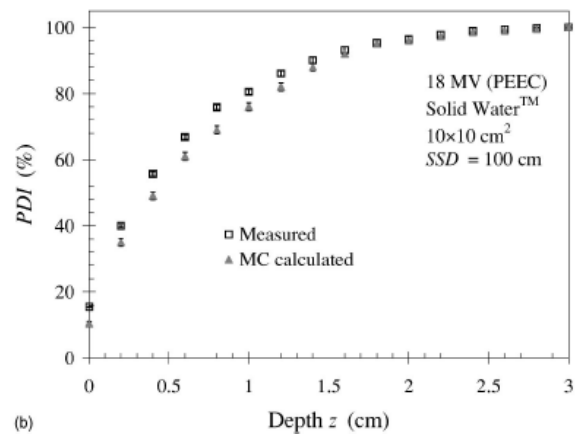
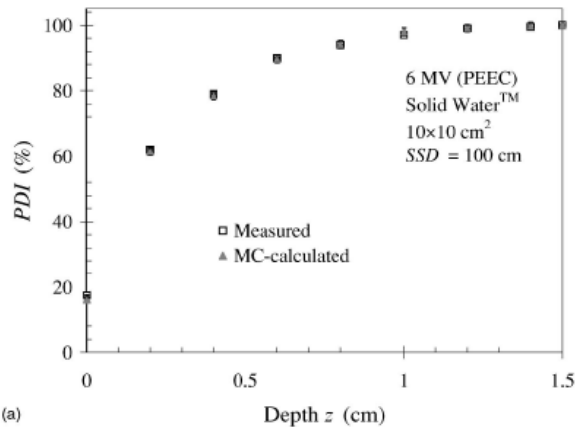


# More Recent Studies of Build-up Dose

## Validation of Monte Carlo calculated surface doses for megavoltage photon beams

Wamied Abdel-Rahman,<sup>a)</sup> Jan P. Seuntjens, Frank Verhaegen,  
François Deblois, and Ervin B. Podgorsak  
*Department of Medical Physics, McGill University Health Centre, 1650 Avenue Cedar, Montreal,  
Quebec, Canada H3G 1A4*

(Received 29 June 2004; revised 20 September 2004; accepted for publication 19 October 2004;  
published 4 January 2005)



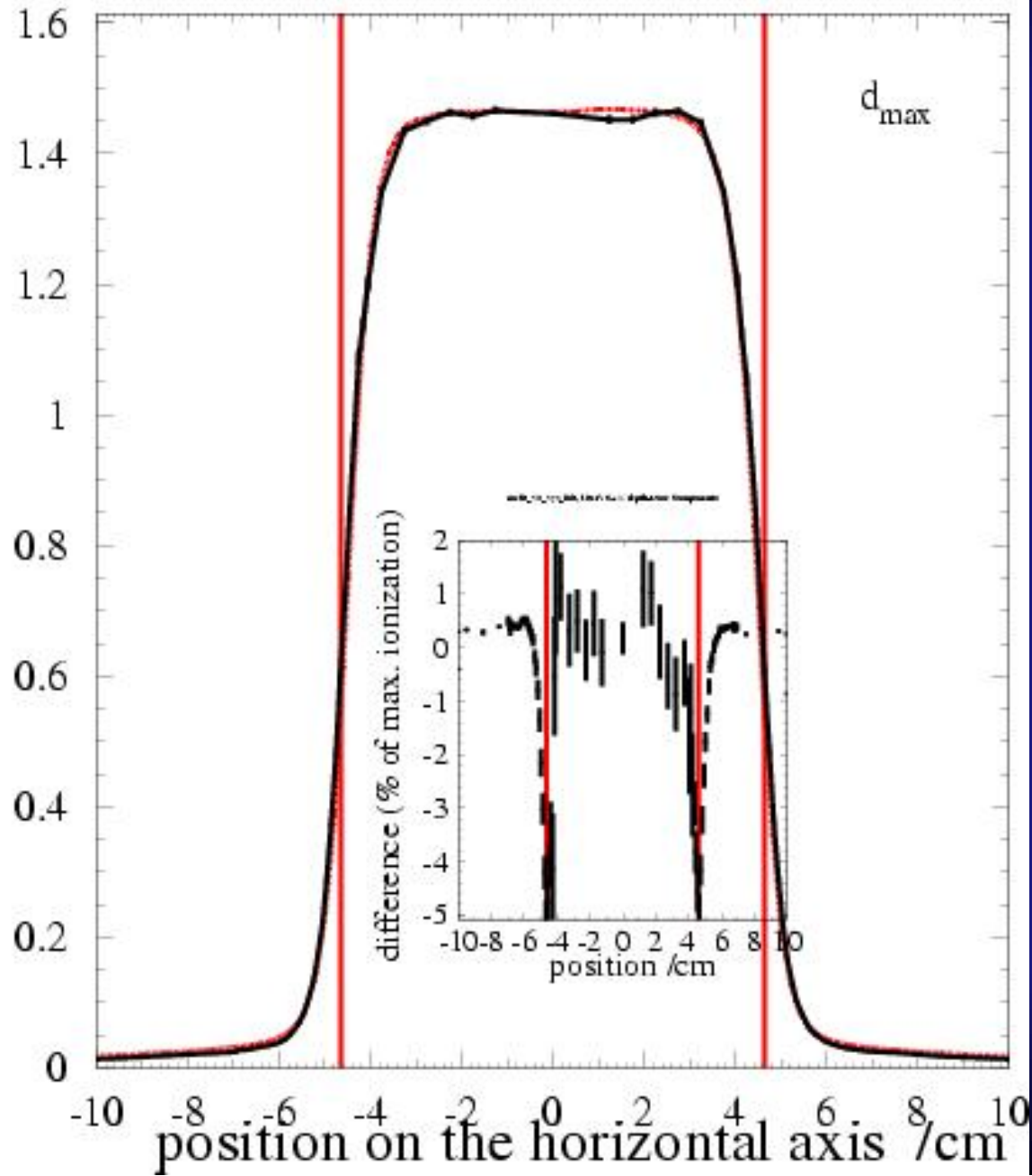
### Ruled out:

- unknown electron source in the head model
- contaminating neutrons;
- faulty cross section data;
- $(x,p)$  reactions.

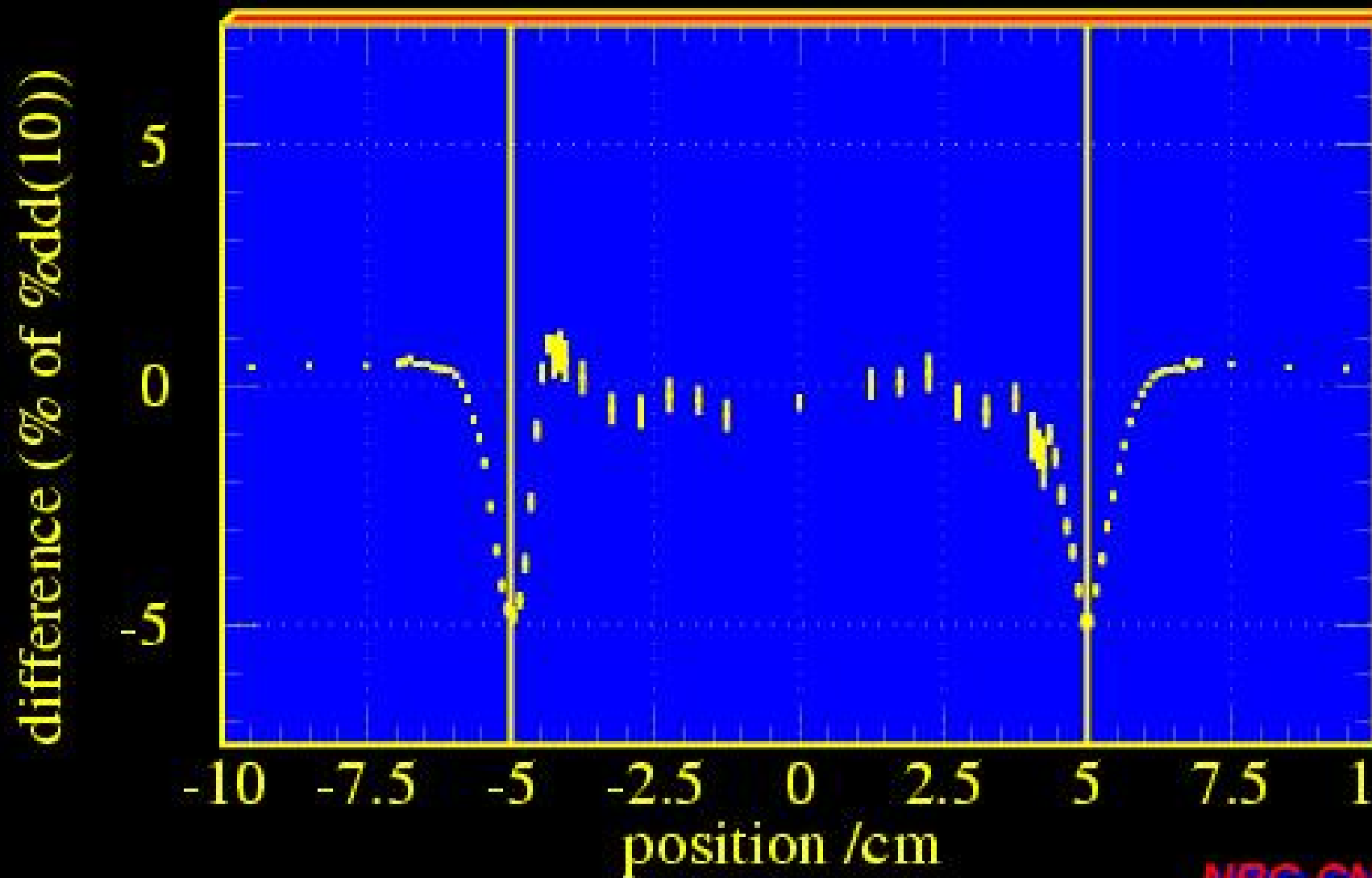
- Showed a simplified model of triplet production can affect the build-up dose for the 18 MV beam
- But still not sufficiently



ionization normalized at 10 g/cm<sup>2</sup> on central axis

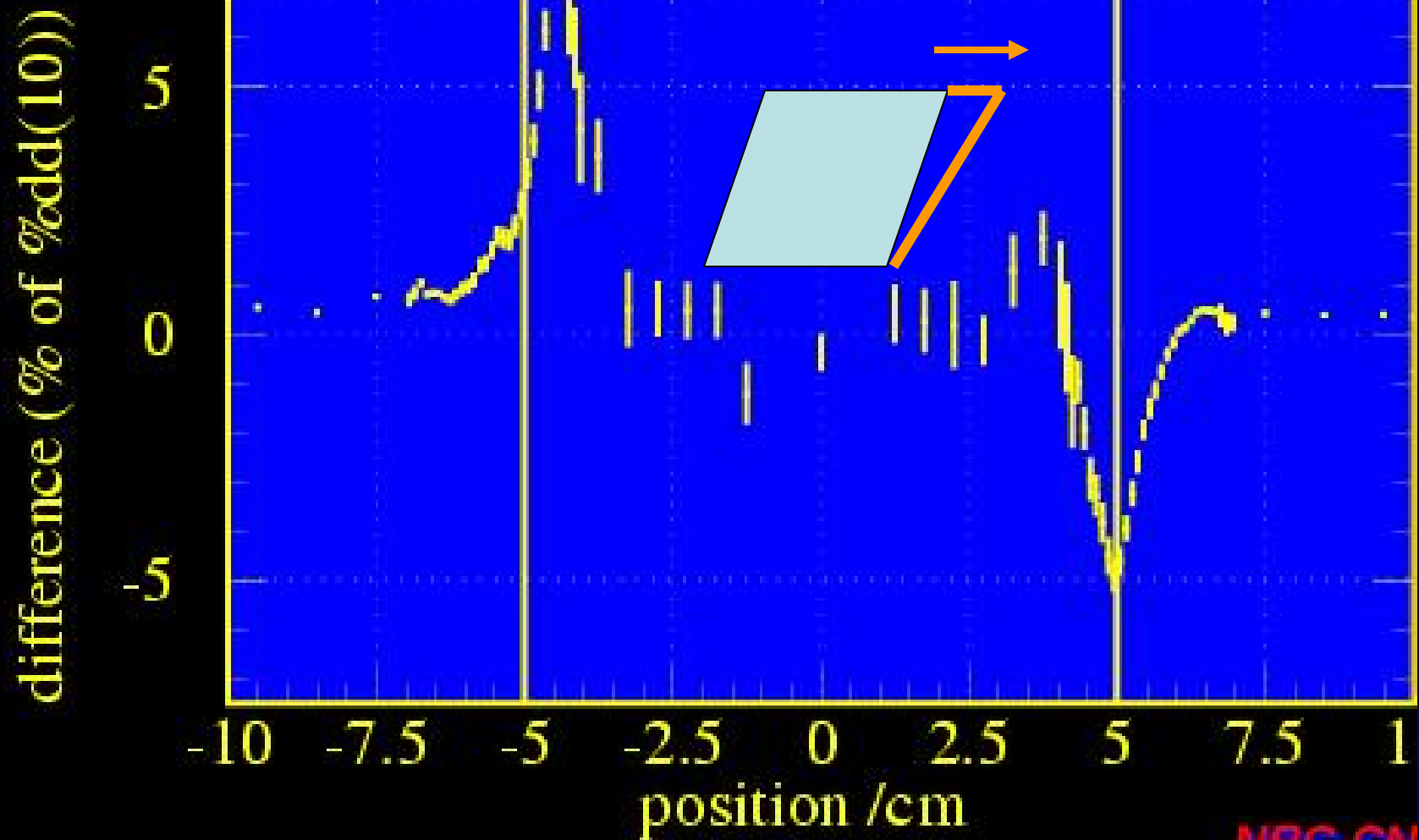


Our best estimate of the jaw settings





Closed the left hand jaw by only 0.5 mm

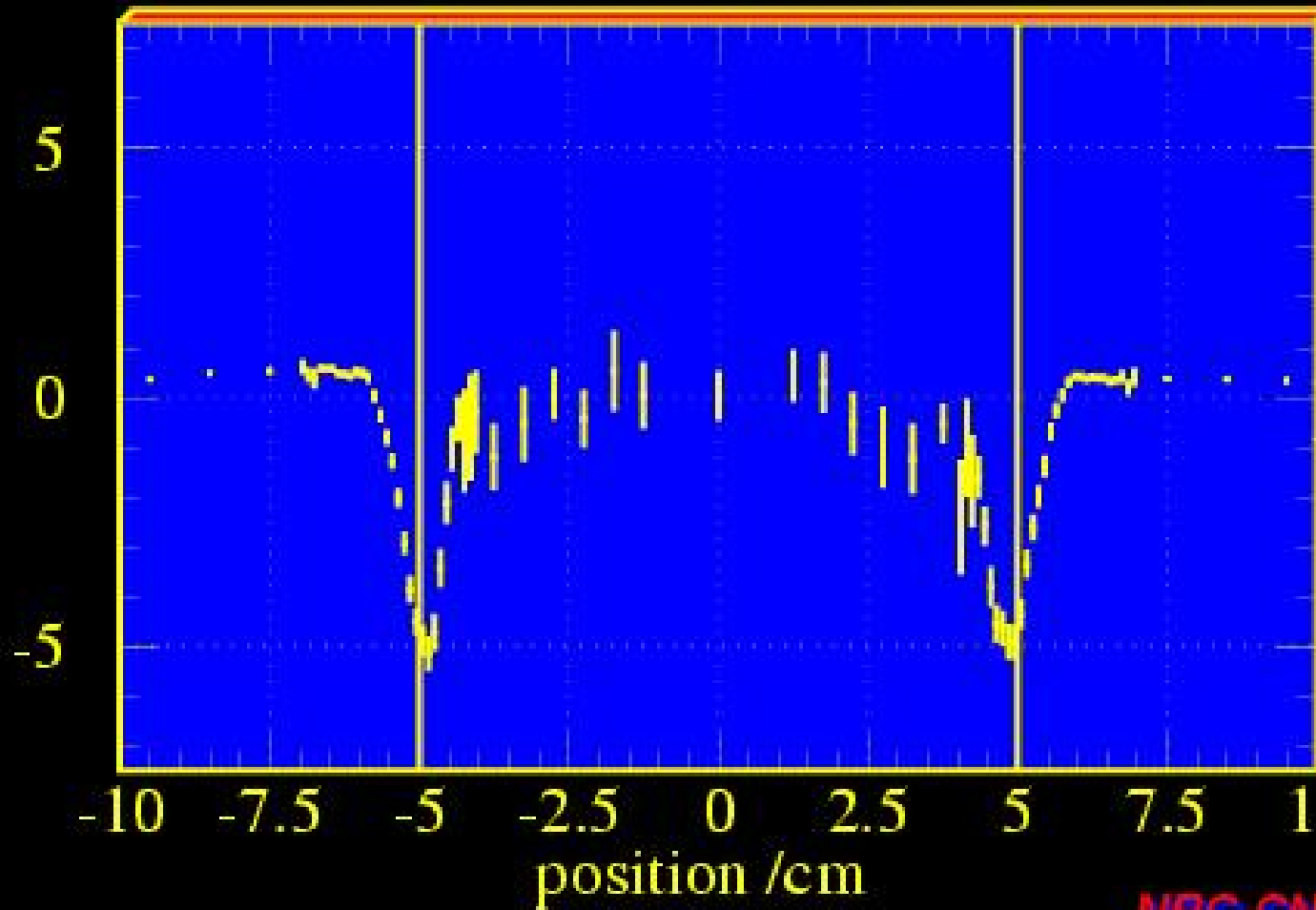


NRC-CN

AGH

Reduced the FWHM of the e- beam by 0.5 mm

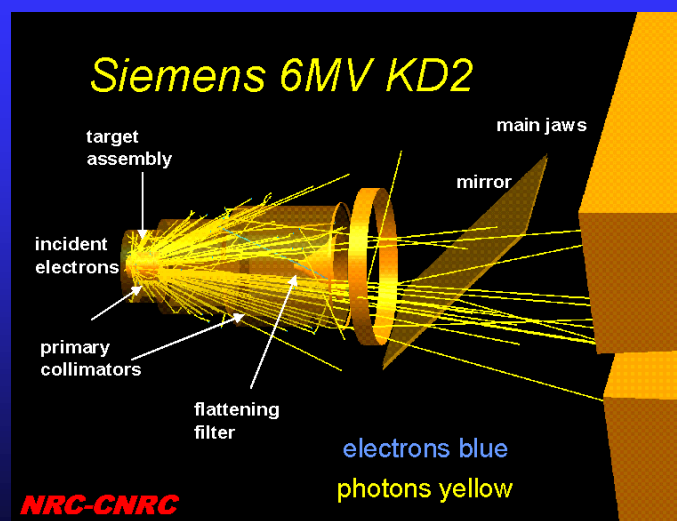
difference (% of  $\%dd(10)$ )



NRC-CN



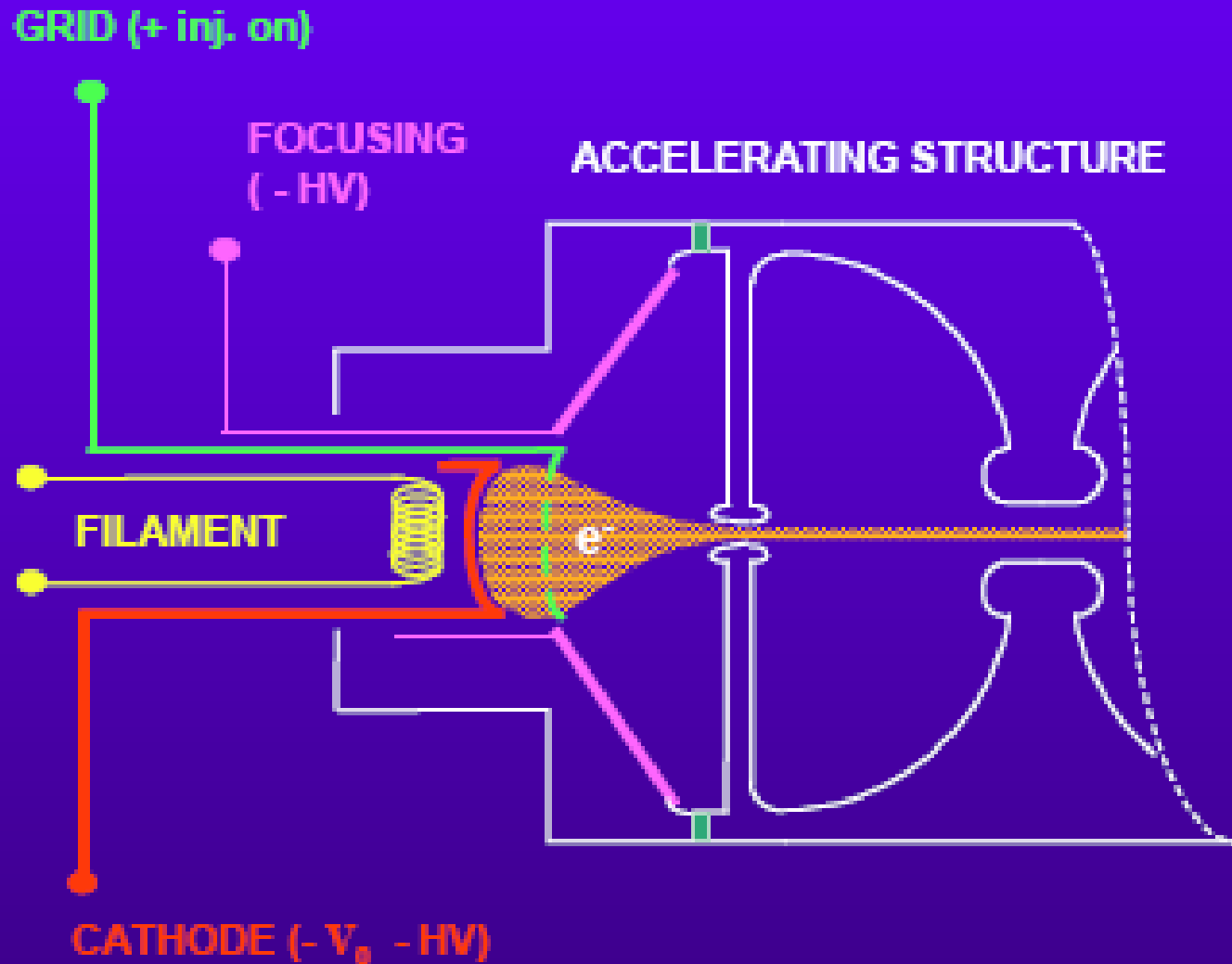
# Sensitivity of Measurable Beam Characteristics to the Model of the Accelerator



# Influence of Initial Electron Characteristics



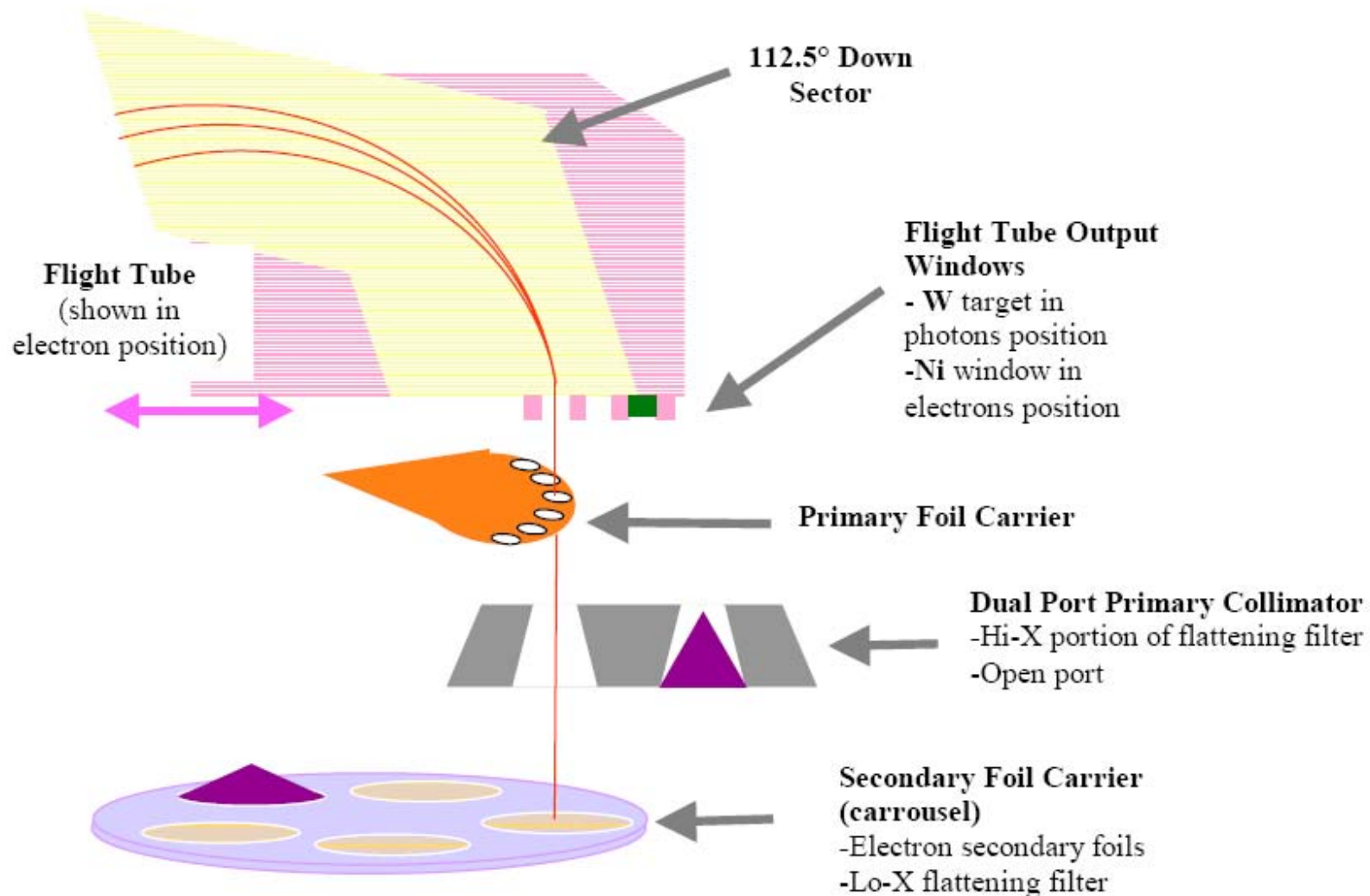
# Where electrons start ...



Courtesy of Tim Waldron, M. D. Anderson



# ... where electrons continue ...

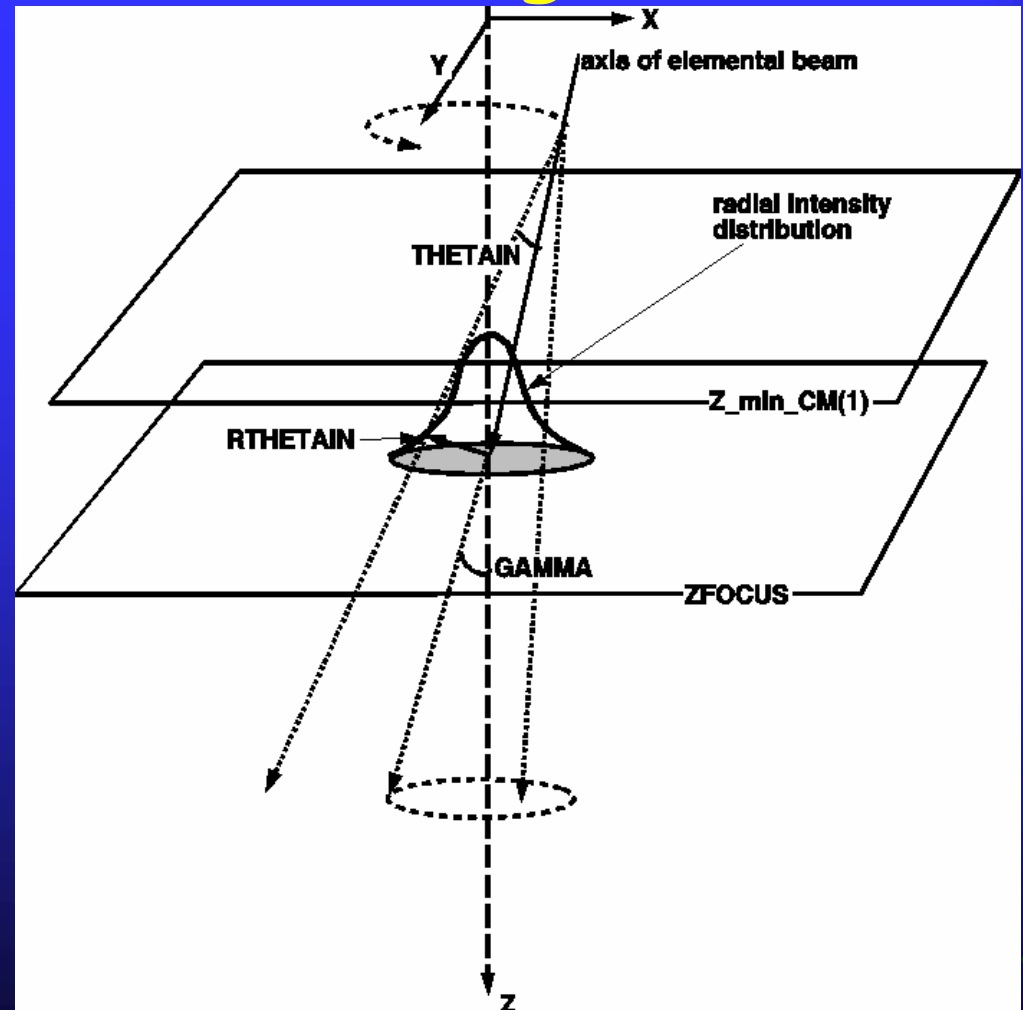


Courtesy of Tim Waldron, M. D. Anderson

AGH

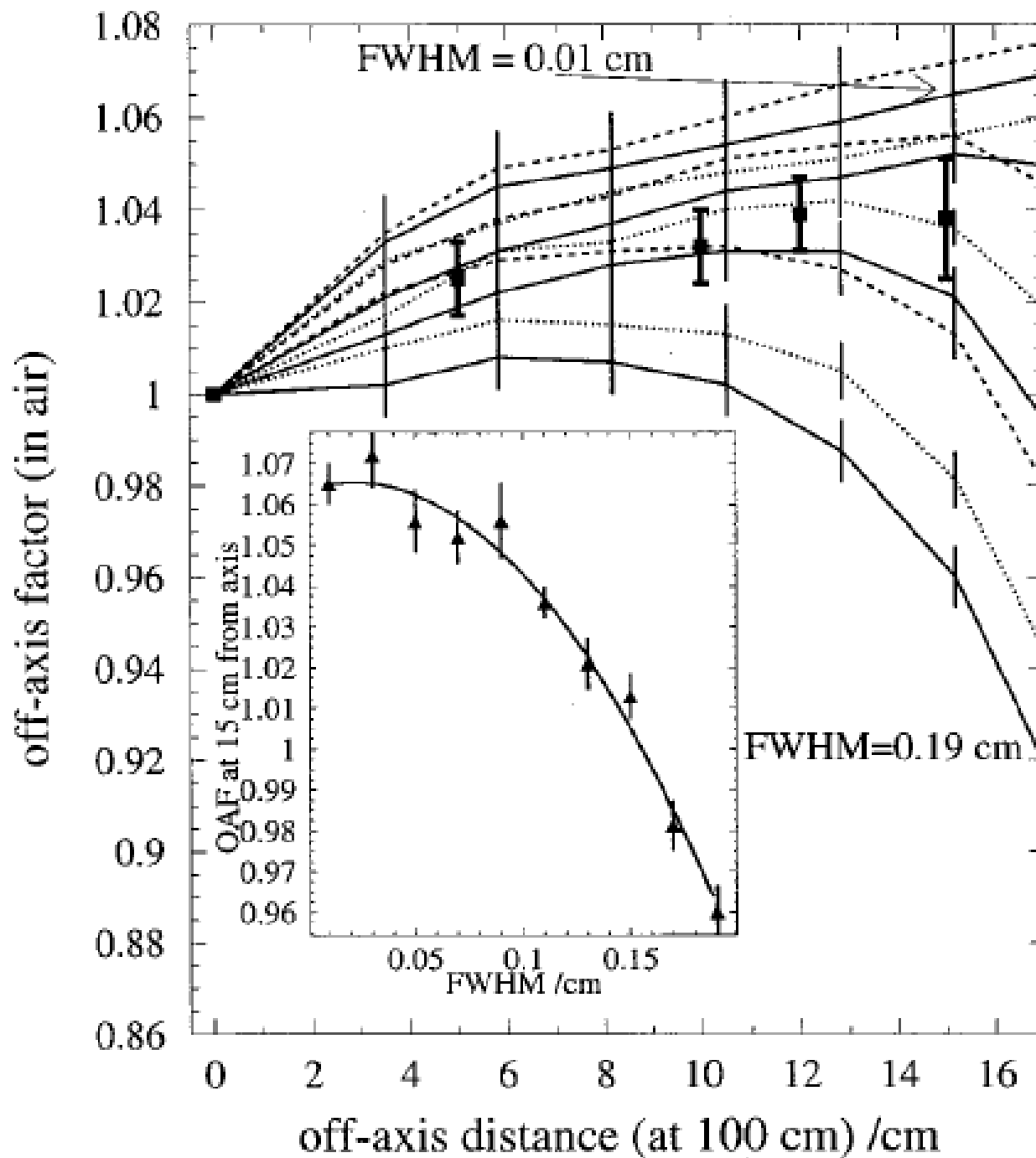
# Radial Distribution of electron beam-on-target

- Not typically provided confidently by manufacturers
- The user may end up deriving it from dosimetric measurements.
- Mainly influences the off-axis factors









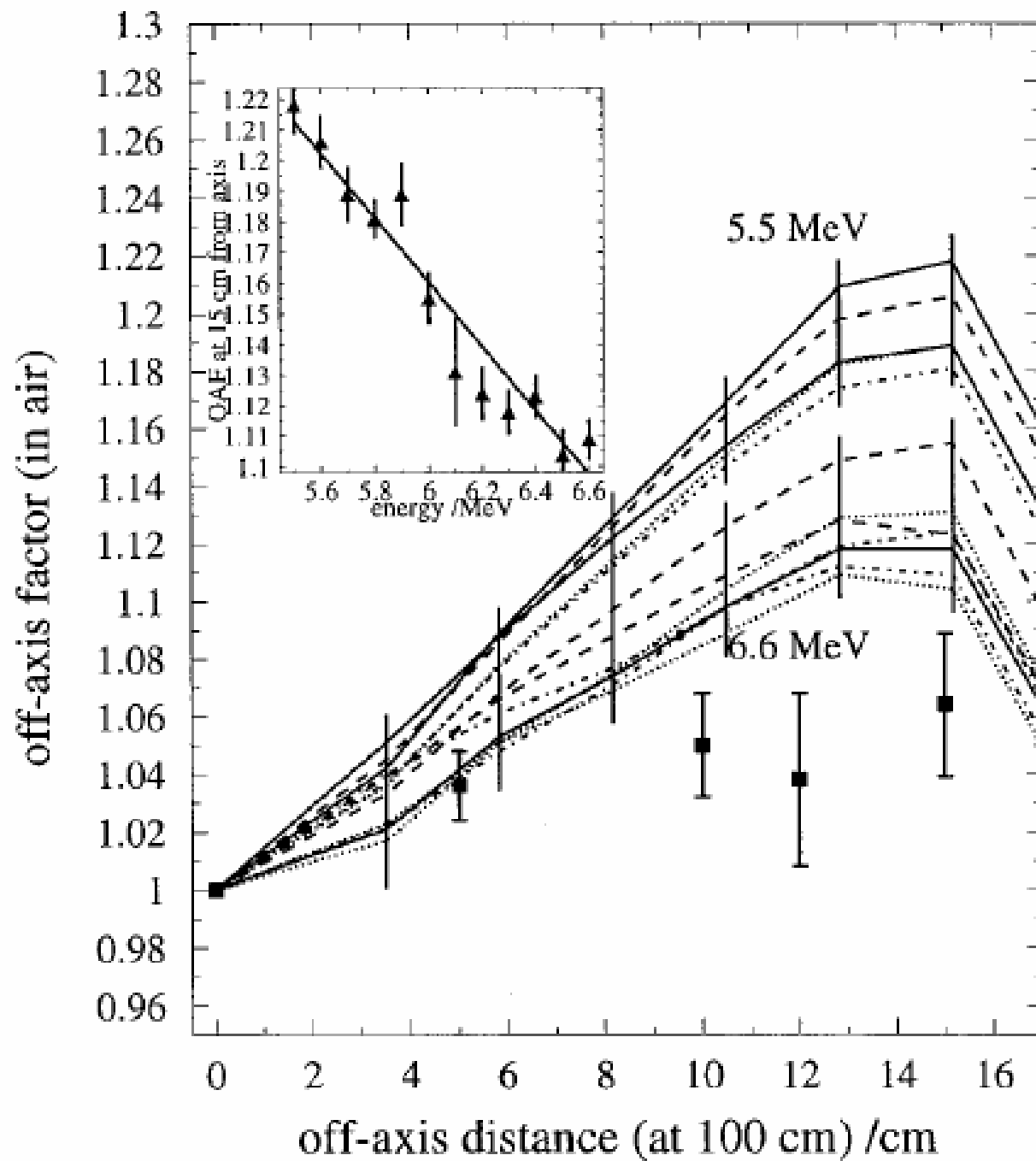
Variation of  
OAFs with  
the FWHM of  
the incident  
electron beam  
radial  
intensity  
distribution

Medical Physics, Vol. 29,  
No. 3, March 2002



# *Energy and Energy Distribution of electron beam-on-target*

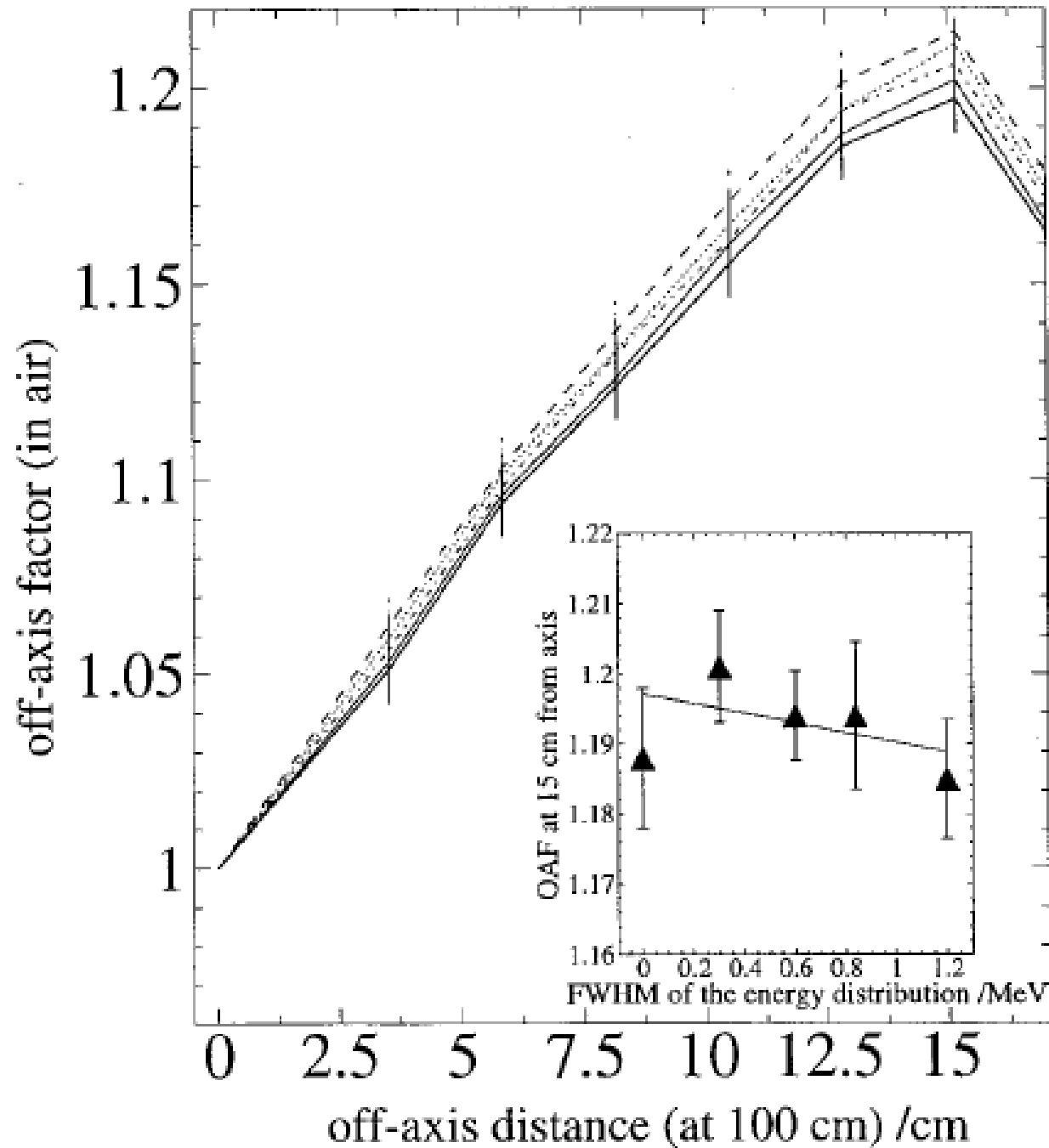
- Both DD and OAF are sensitive to the energy variation
- As the energy increases the horns reduce
- Varying the FWHM of the energy distribution of the electron beam-on-target from 0-20% not observable on the calculated OAFs and very small effect on the depth-dose curves
- The effect of asymmetrical electron energy spectrum on the photon build-up DD although relatively small, is observable (Sheikh-Bagheri and Rogers 2002a).



The effect of  
Mean Energy  
of the electron  
beam-on-target,  
on the in-air  
OAF

Medical Physics, Vol. 29, No. 3,  
March 2002

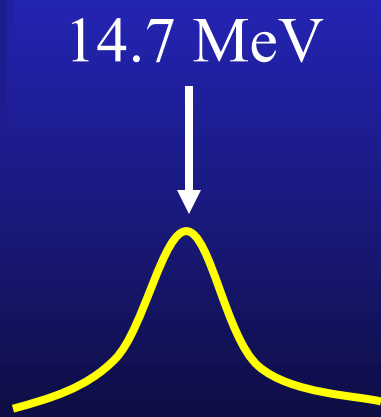
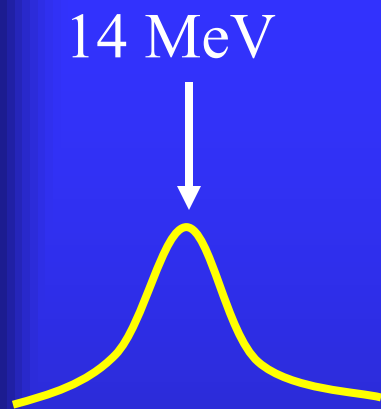




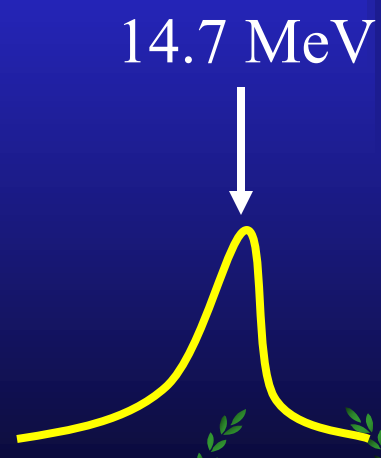
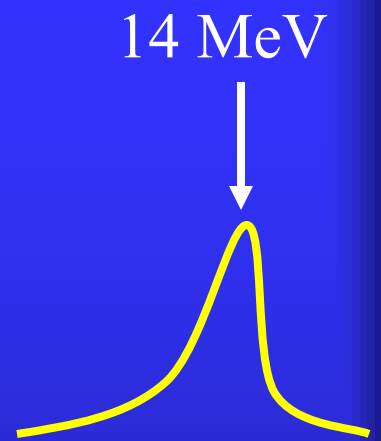
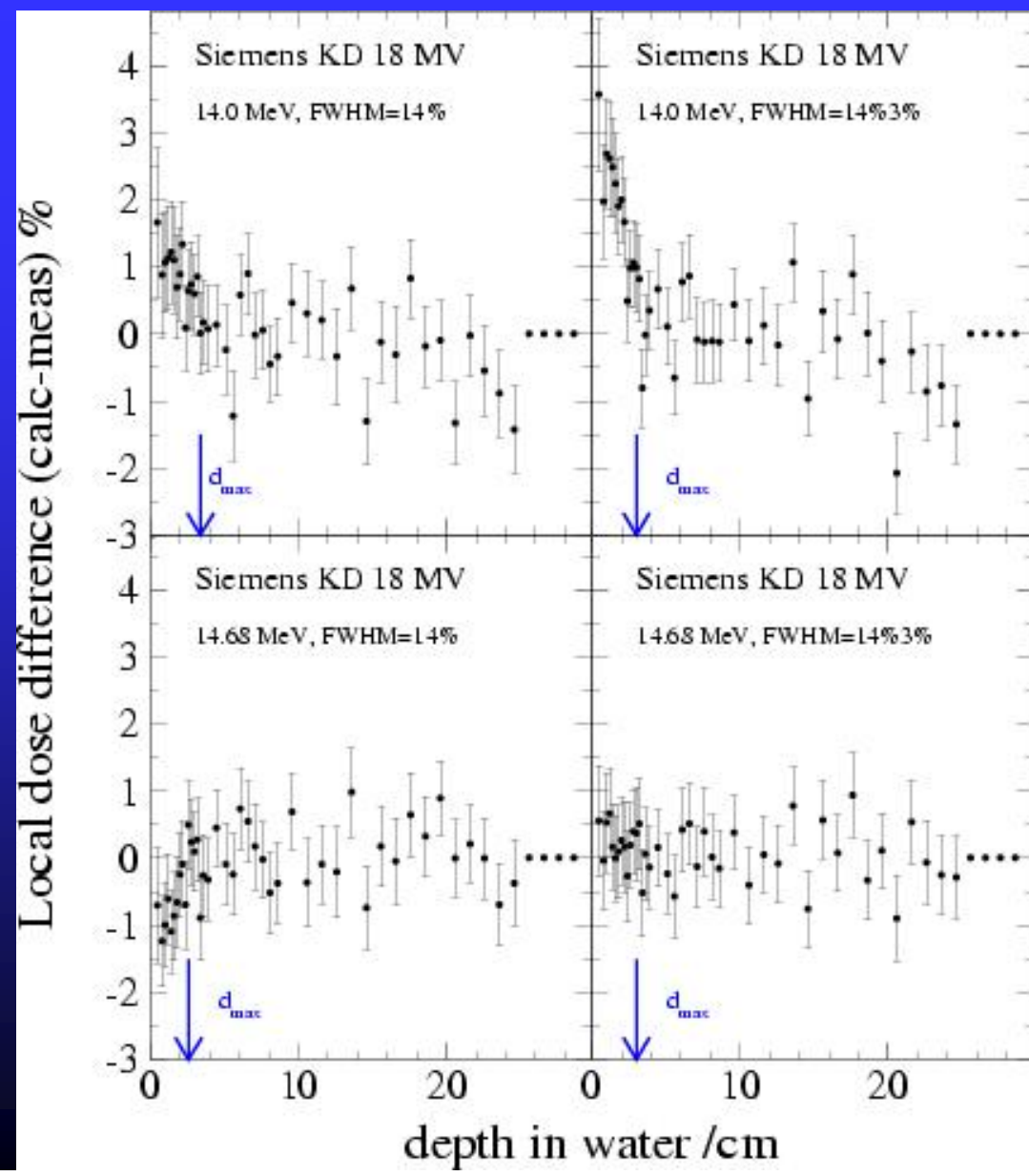
## Variation of OAFs with the energy spread of the incident electron beam

Medical Physics, Vol. 29,  
No. 3, March 2002

# Are even finer details of the e- beam energy distribution observable?



Medical Physics, Vol. 29,  
No. 3, March 2002

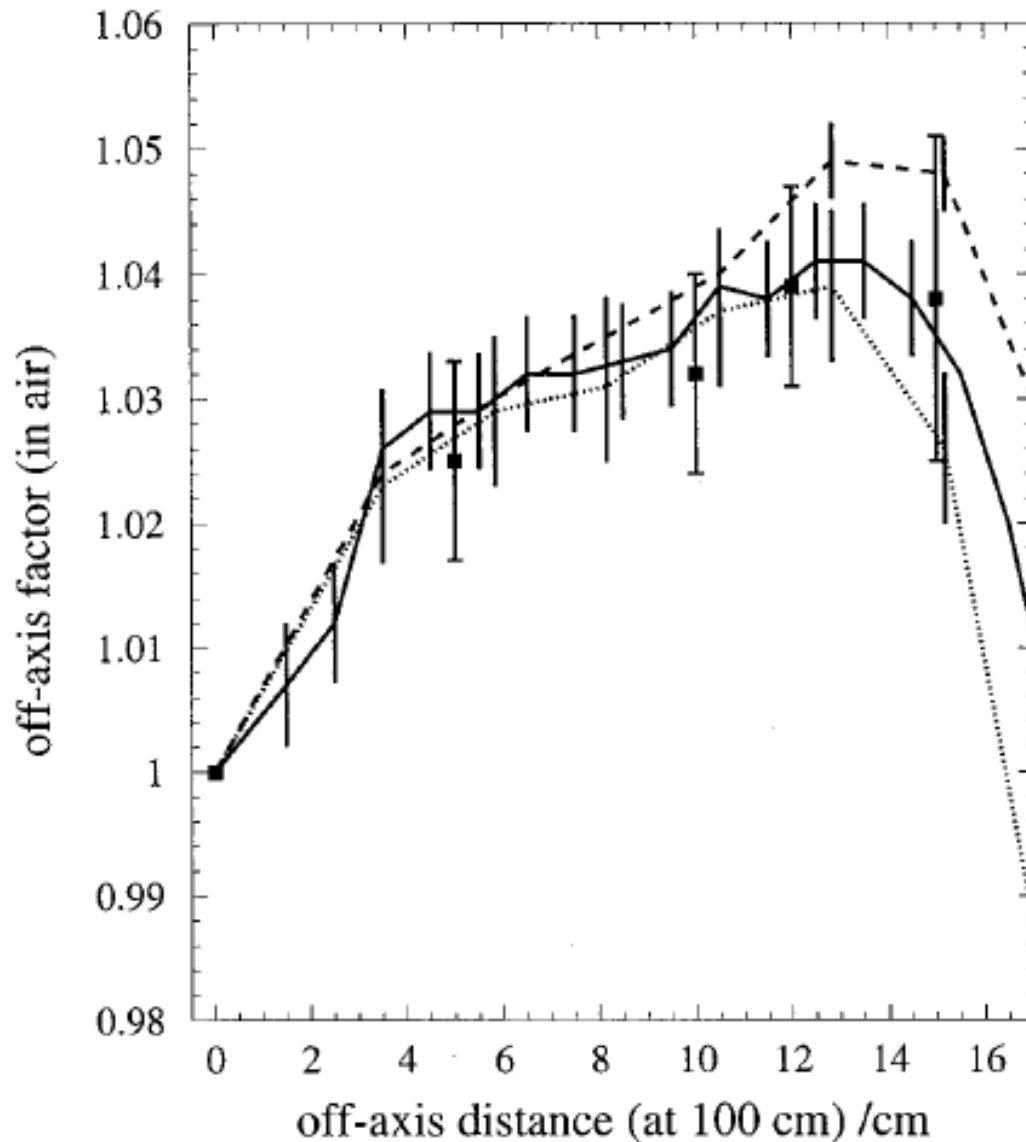


# Influence of Accelerator components

## ... the target

- Keall et al. (2003)
- Increasing the target density hardens the 6 MV DD and softens the 18 MV DD
- Small change in density affects the DD, but not significantly
- Varying the density from 18 to 17 g/cm<sup>3</sup> → 1.7% difference in dose profiles for the 6 MV and 0.3% for the 18 MV beams
- Sheikh-Bagheri et al. (2000 and 2002a)
- The target lateral dimensions not important if the target width is much larger than the lateral spread of electrons in the target or the radius of the upstream opening of the primary collimator
- Otherwise OAFs affected

# ...the primary collimator



Variation of  
OAFs with  
a variation of  
0.01 cm in the  
upstream  
radius of the  
primary  
collimator

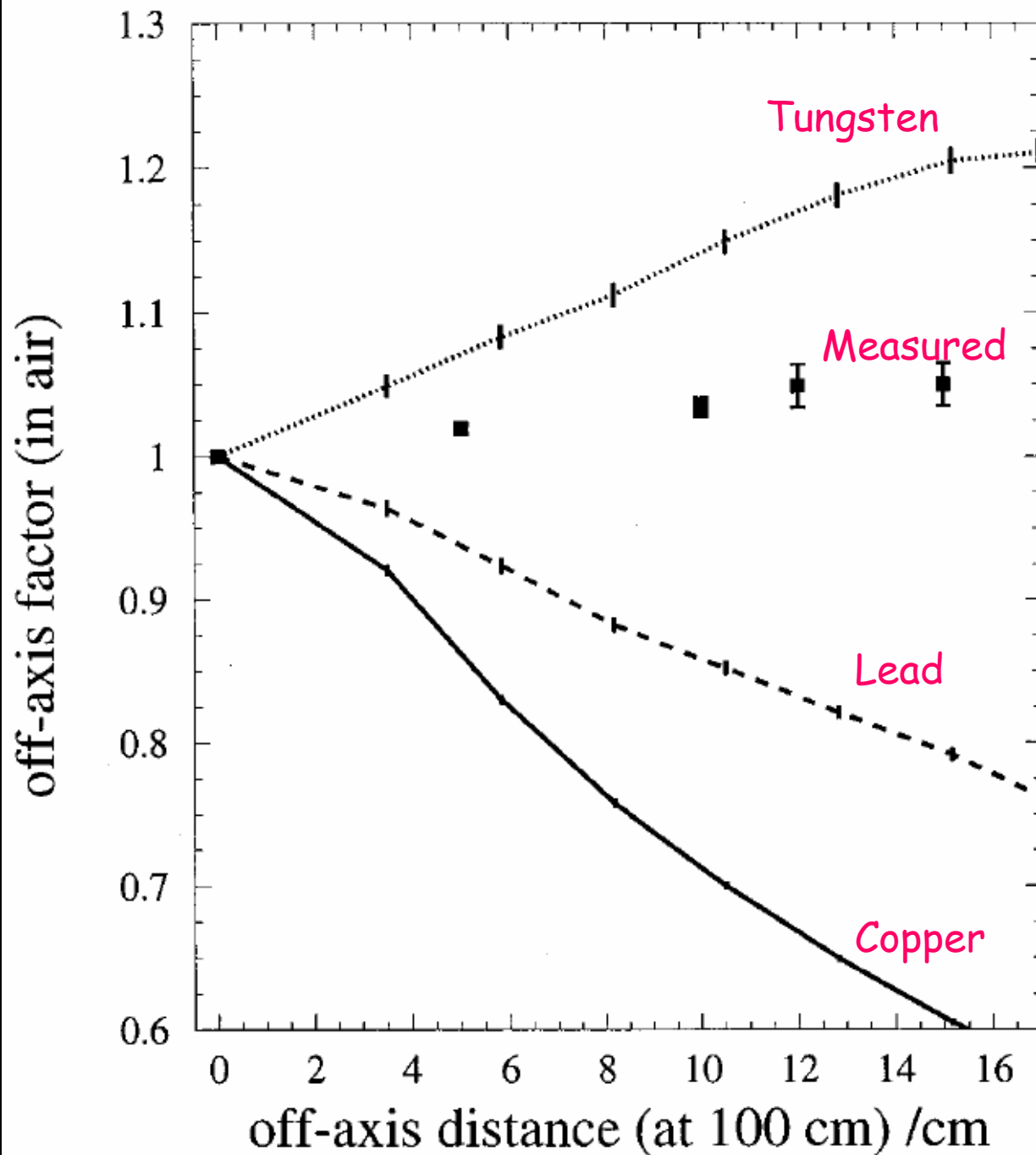
Medical Physics, Vol. 29,  
No. 3, March 2002





## ... the flattening filter

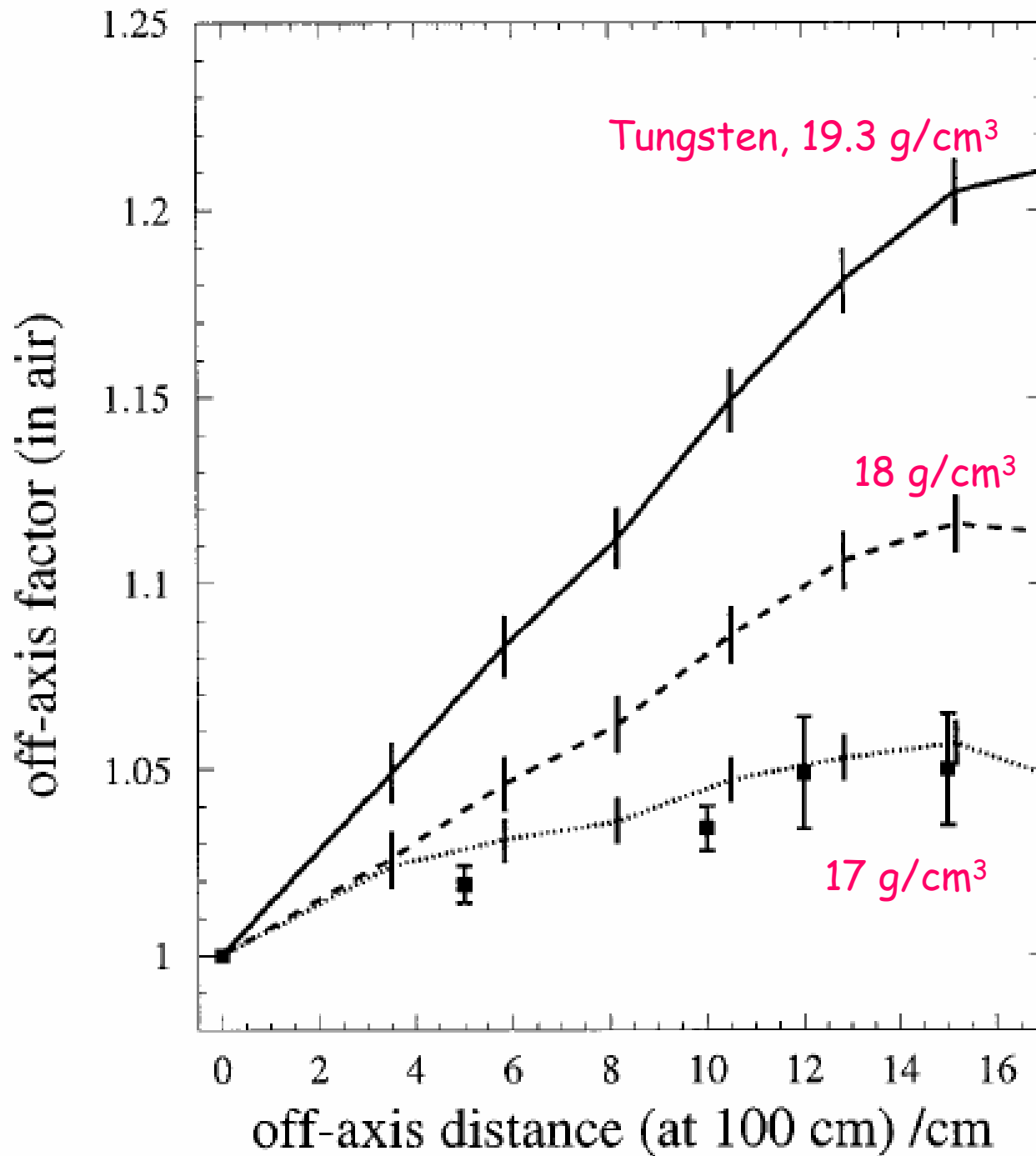
- The manufacturers commonly provide very precise dimensions of the flattening filter.
- Mistakes can happen; blueprint said FF made of Copper
- Density affects the "in-air" and consequently "in-phantom" dose profiles dramatically
- The density of different types of pure W varies by more than  $1 \text{ g/cm}^3$
- Better know the density to better than  $0.25 \text{ g/cm}^3$



## Variation of OAFs with the material of the FF

Medical Physics, Vol. 29,  
No. 3, March 2002





## Variation of OAFs with the density of the FF

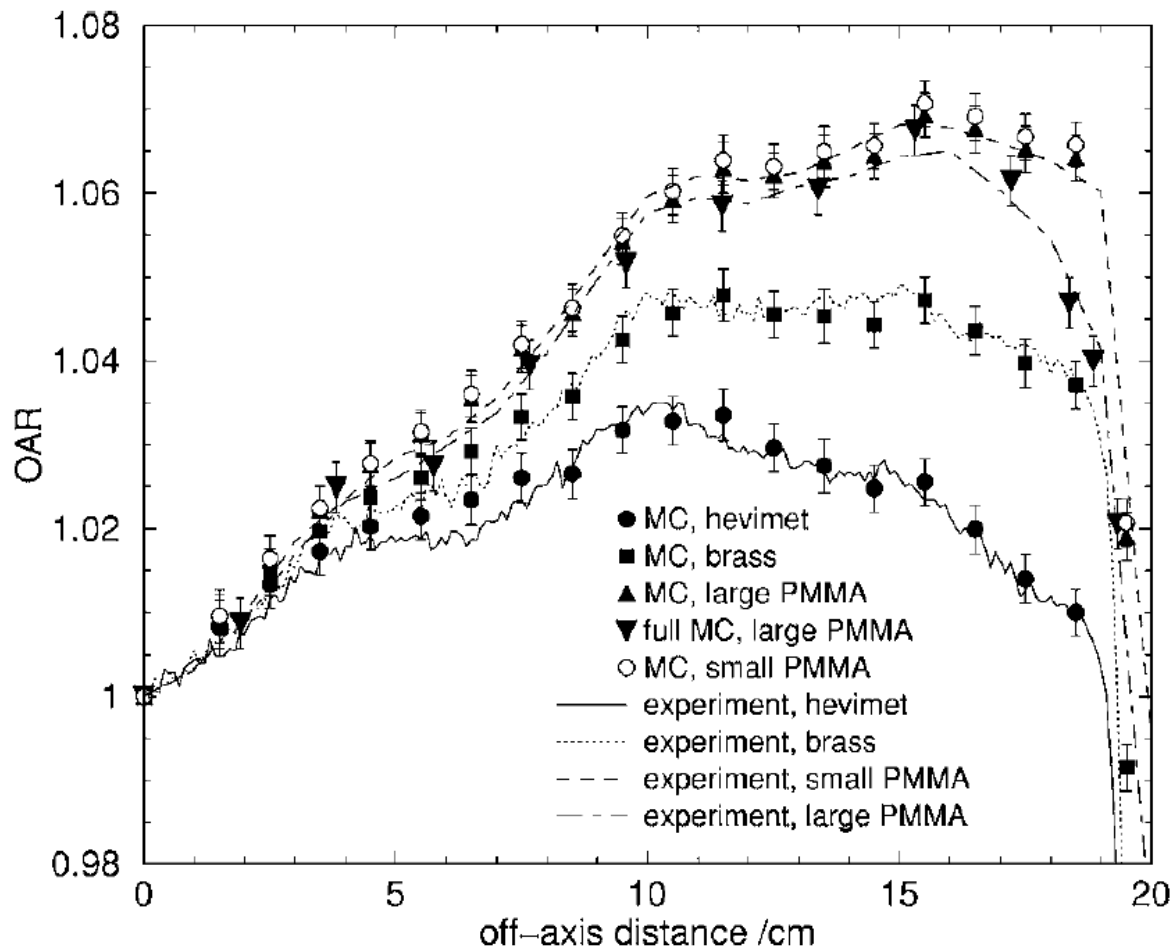
Medical Physics, Vol. 29,  
No. 3, March 2002



## Influence of ion chamber response on in-air profile measurements in megavoltage photon beams

E. Tonkopi,<sup>a)</sup> M. R. McEwen, B. R. B. Walters, and I. Kawrakow  
*Ionizing Radiation Standards, NRC, Ottawa, KIA 0R6, Canada*

(Received 25 April 2005; revised 5 July 2005; accepted for publication 7 July 2005;  
published 26 August 2005)



- investigated the influence of buildup caps on the in-air OAR measurements

- Confirmed the usefulness of in-air OAFs in MC linac modeling

# Facts:

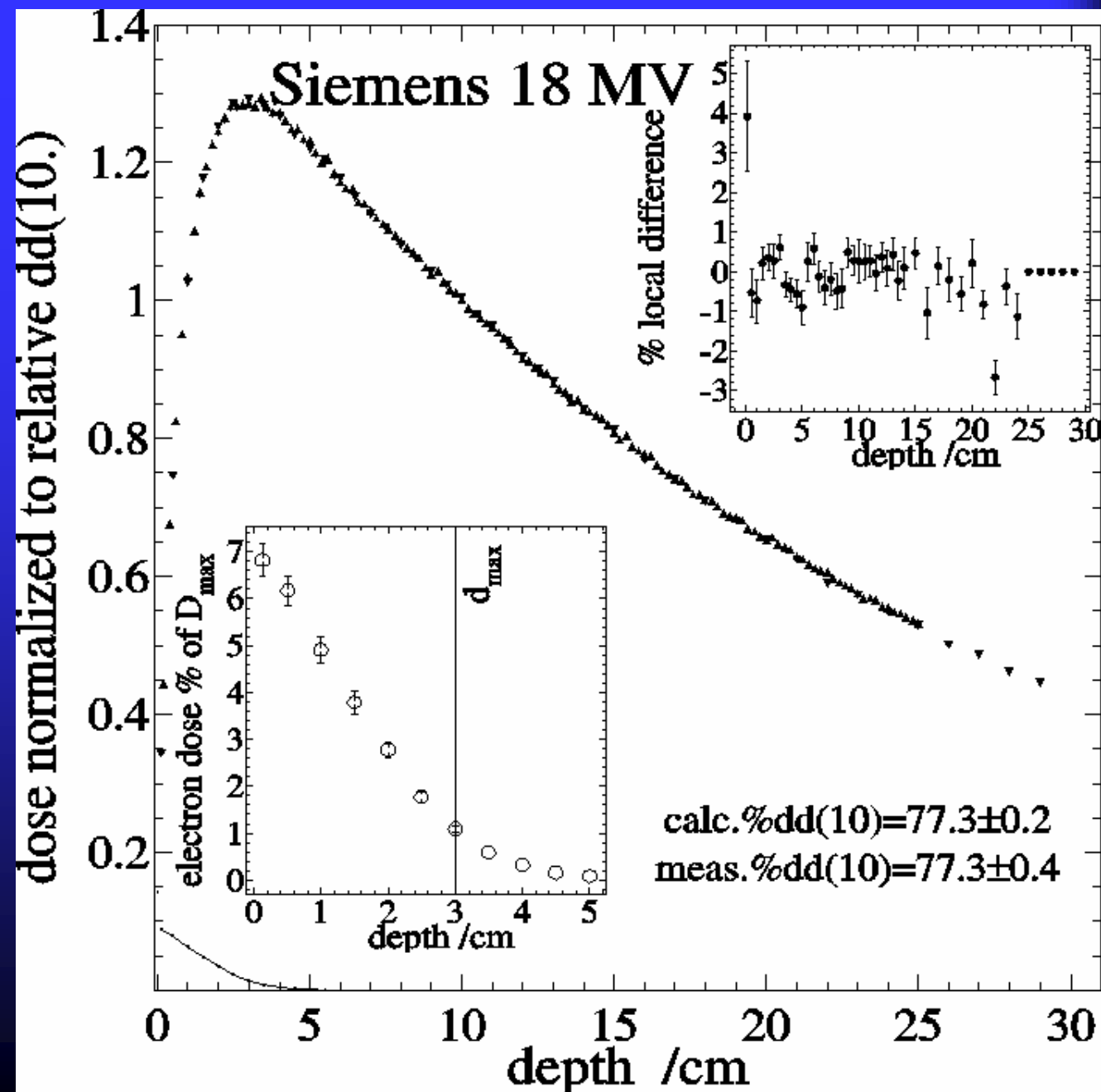
- Both OAF and DD are sensitive to electron beam-on-target energy ...
- The OAFs (and therefore dose profiles) are also sensitive to the electron beam-on-target radial intensity distribution
- However the DD is not

# One approach ...

- First start with a best estimate for both
- Using central-axis relative depth-doses find → the energy of the electron beam and its energy distribution
- Then use off-axis factors to determine the radial intensity distribution and fine tune the electron beam energy
- Note: the accuracy of the derived model parameters is directly affected by the accuracy of the measured dosimetric data

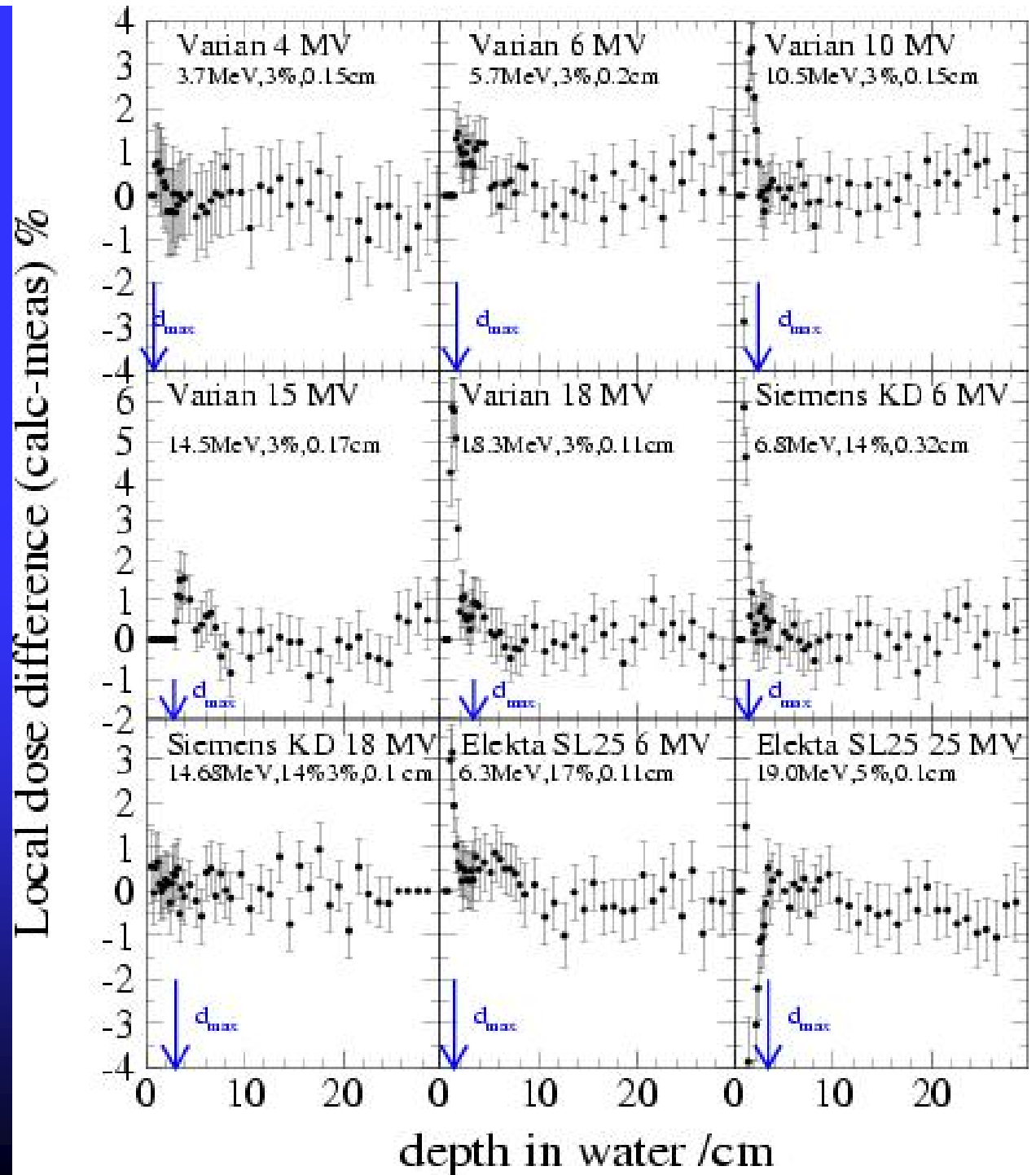
# Comparison of the calculated and measured PDD data.

MC Calculated (◆)  
Siemens measured (♦)



Diff between  
calc and meas  
PDDs

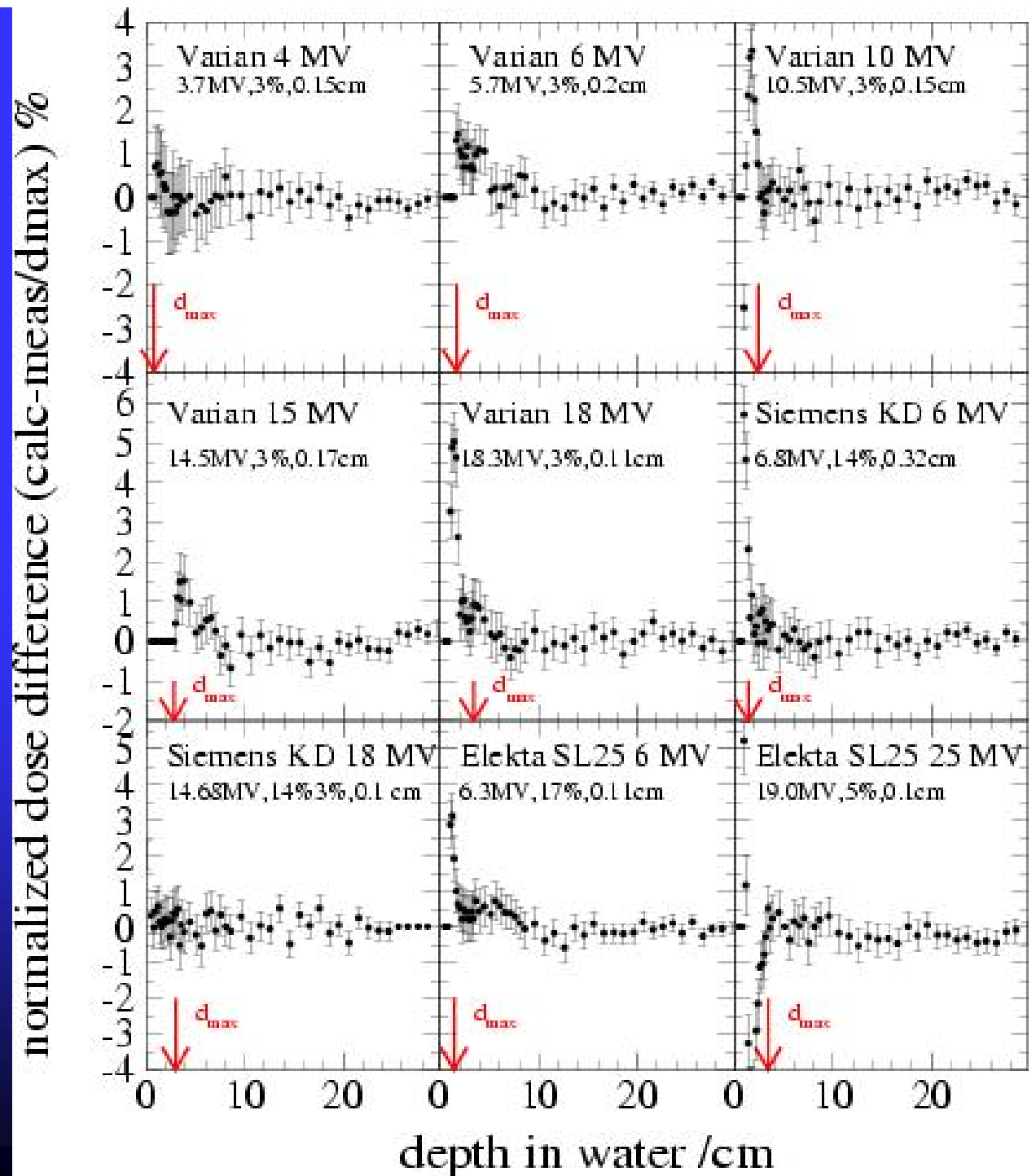
Local  
dose difference





Diff between  
calc and meas  
PDDs

Normalized  
to  $D_{max}$



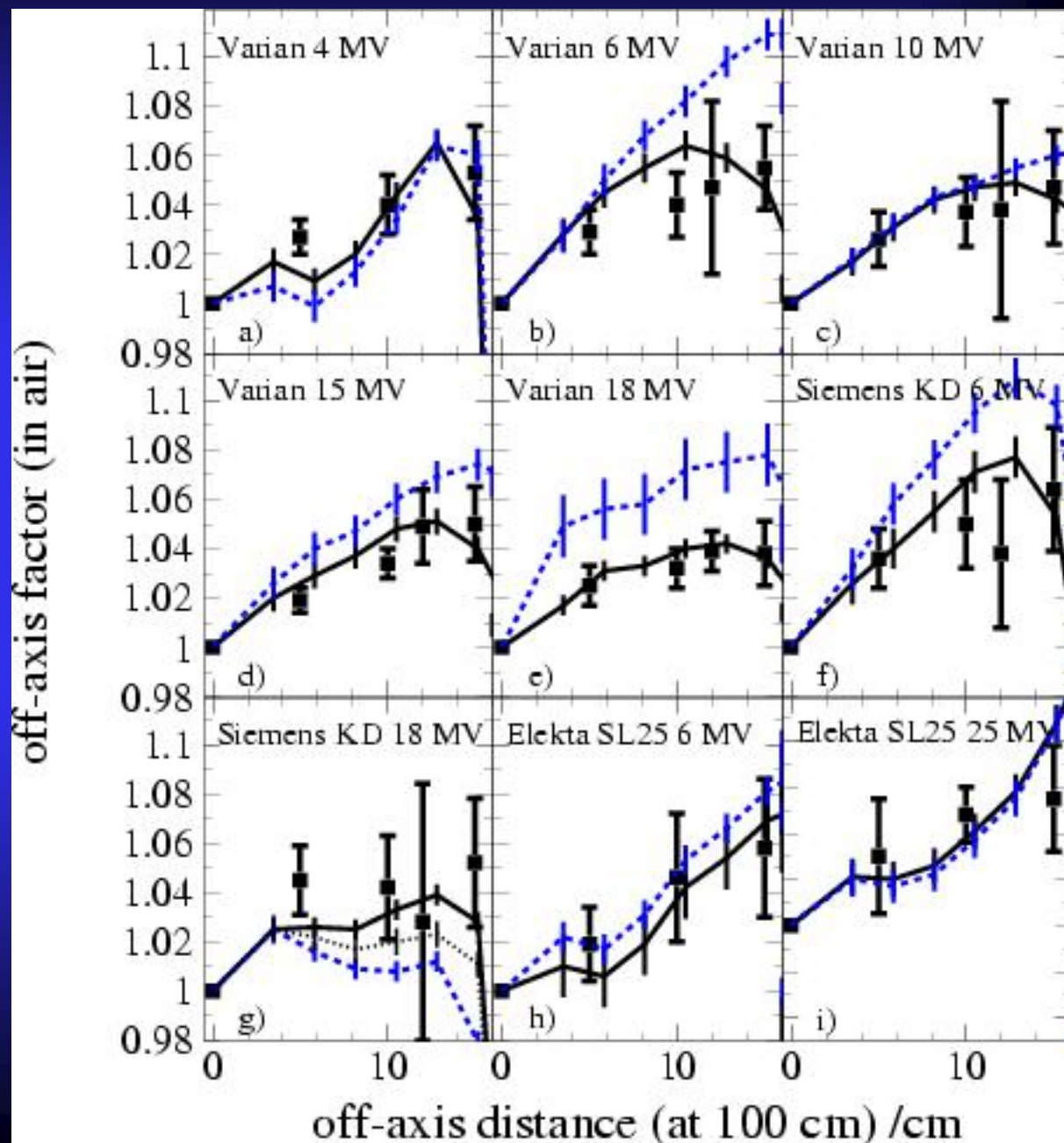
# Calculated and Measured In-Air Off-Axis Factors

Solid lines:  
derived  
parameters

Blue-dashed:  
suggested  
parameters

Symbols: TG-46

Medical Physics, Vol. 29, No. 3,  
March 2002



## Comparison of the derived and the manufacturer suggested electron beam characteristics of some commercial medical linear accelerators

LINAC	Nominal accelerating potential (MV)	Suggested electron energy (MeV) (and spread %) (Manufacturer)	Derived electron energy (MeV) (and spread %)	Nominal electron beam FWHM (cm)	Derived electron beam FWHM (cm)
Varian Clinac low-energy	4	4 (3%)	3.7 (3%)	0.1	0.15
Varian Clinac high-energy	6	6 (3%)	5.7 (3%)	0.1	0.2
	10	10 (3%)	10.5 (3%)	0.1	0.15
	15	15 (3%)	14.5 (3%)	0.1	0.17
	18	18 (3%)	18.3 (3%)	0.1	0.11
Philips SL25	6	6 (17%)	6.3 (17%)	0.1	0.11
	25	19 (5%)	19.0 (5%)	0.1	0.10
Siemens KD	6	5.53 (14%) -> <b>6.6</b>	6.8 (14%)	0.2	0.32
	18	12.87 (14%) -> <b>14.68</b>	14.7 (14%)	0.2	0.10

# Important to model ... when benchmarking

- Exact electron beam energy
- FWHM of the electron beam intensity distribution
  - the details of the shape to a lesser extent
- Geometrical details ... of course
- Material and density of the flattening filter
- Exact jaw settings
- Exact angle of incidence of the e- beam on target
- Finite size of detector (build-up dose)
- The above list not exhaustive ...

## ... not as important ...

- Electron beam divergence ( $< 5$  mrad)
- Exact FWHM of electron beam energy ( $< 5$  %)
  - the details of the shape to some extent
- Electron multiple scattering in target
- Finite size of detector (for a reasonably small ion chamber)
- Variation of  $SPR_{\text{air}}^{\text{water}}$  with depth or laterally
- Energy response of the ion chamber

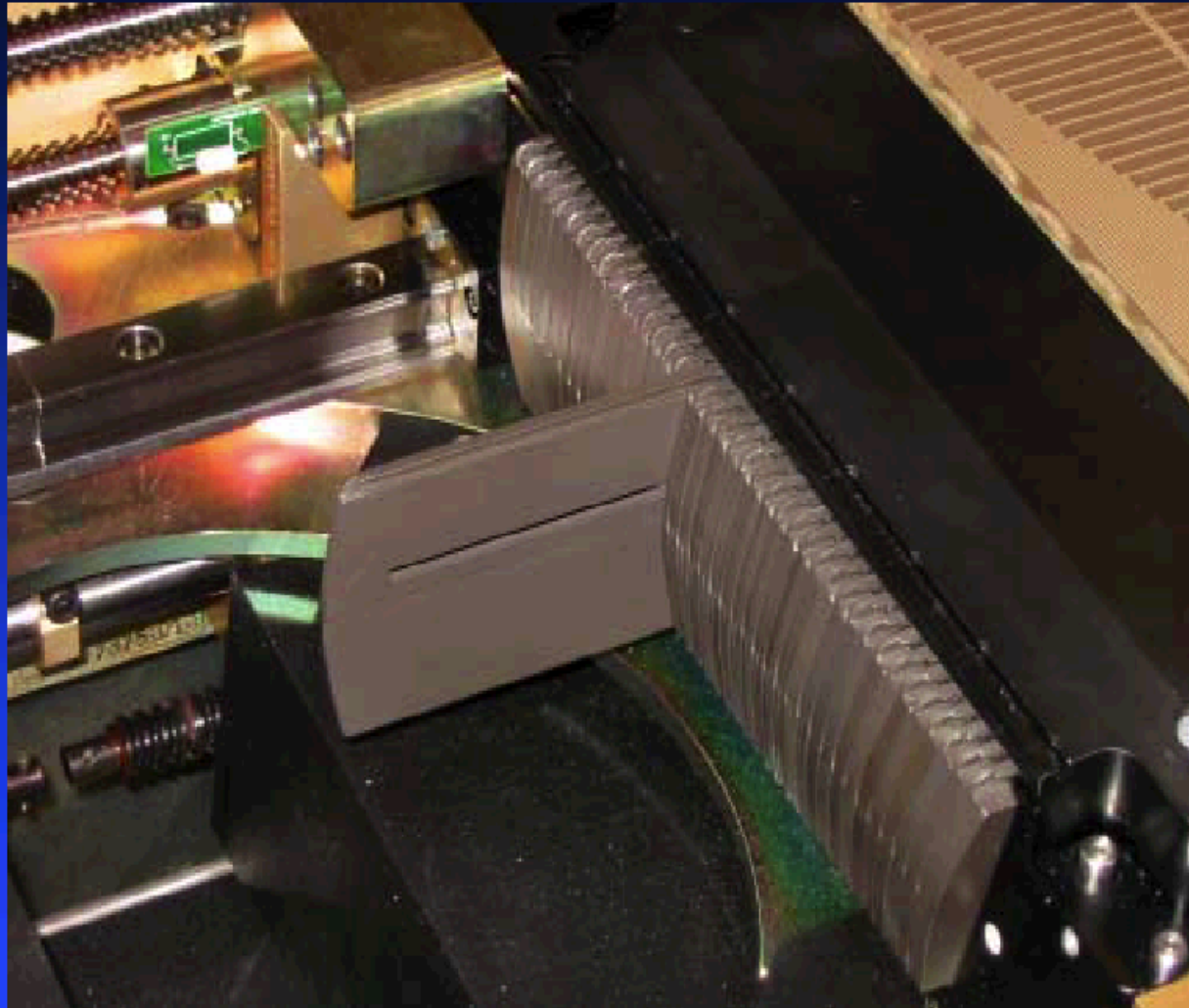
# Modeling MLCs in Detail

Examples:

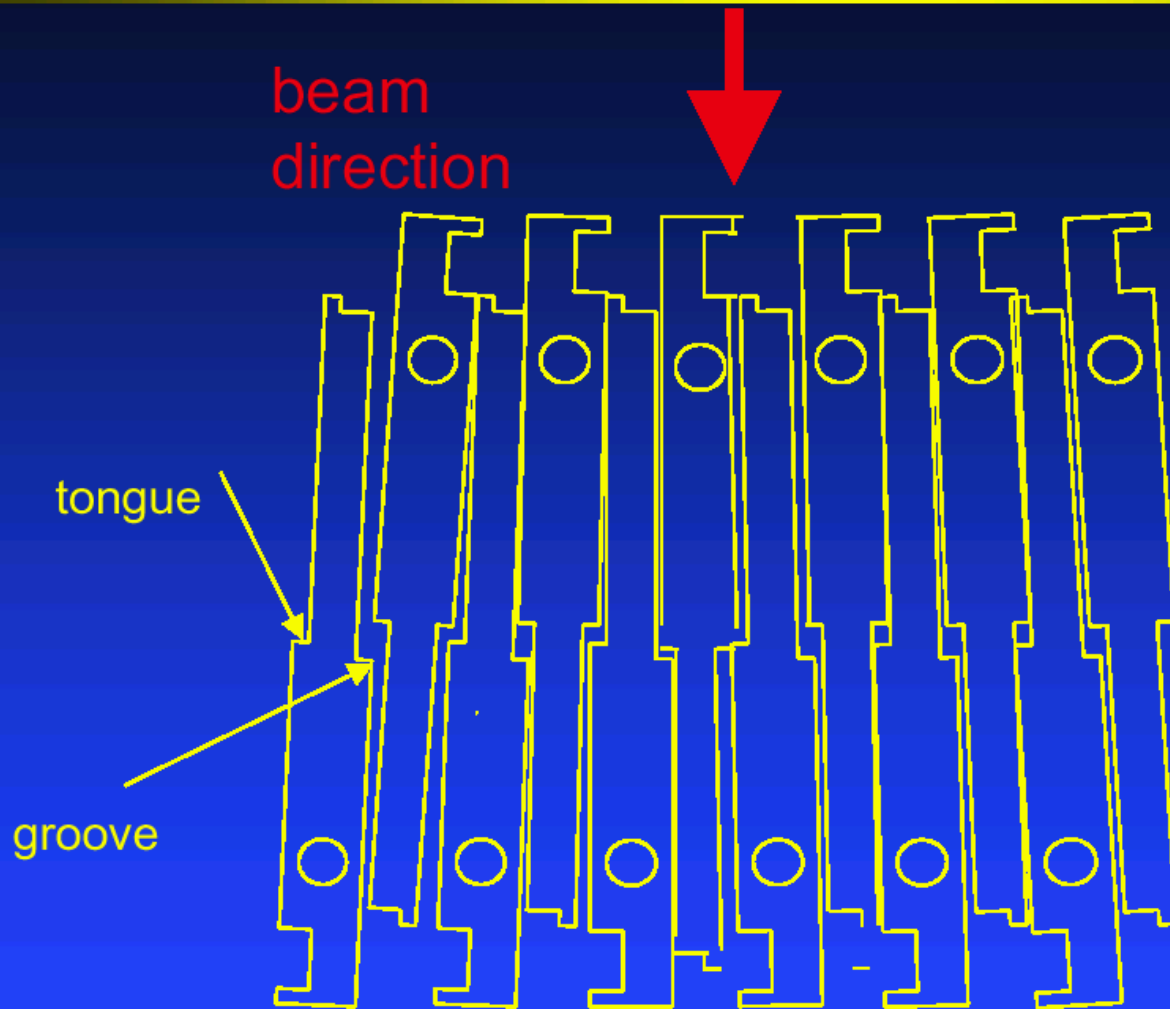
McGill  
NOMOS



# Varian Millennium 120 leaf MLC



# Millennium MLC - Inner Leaves

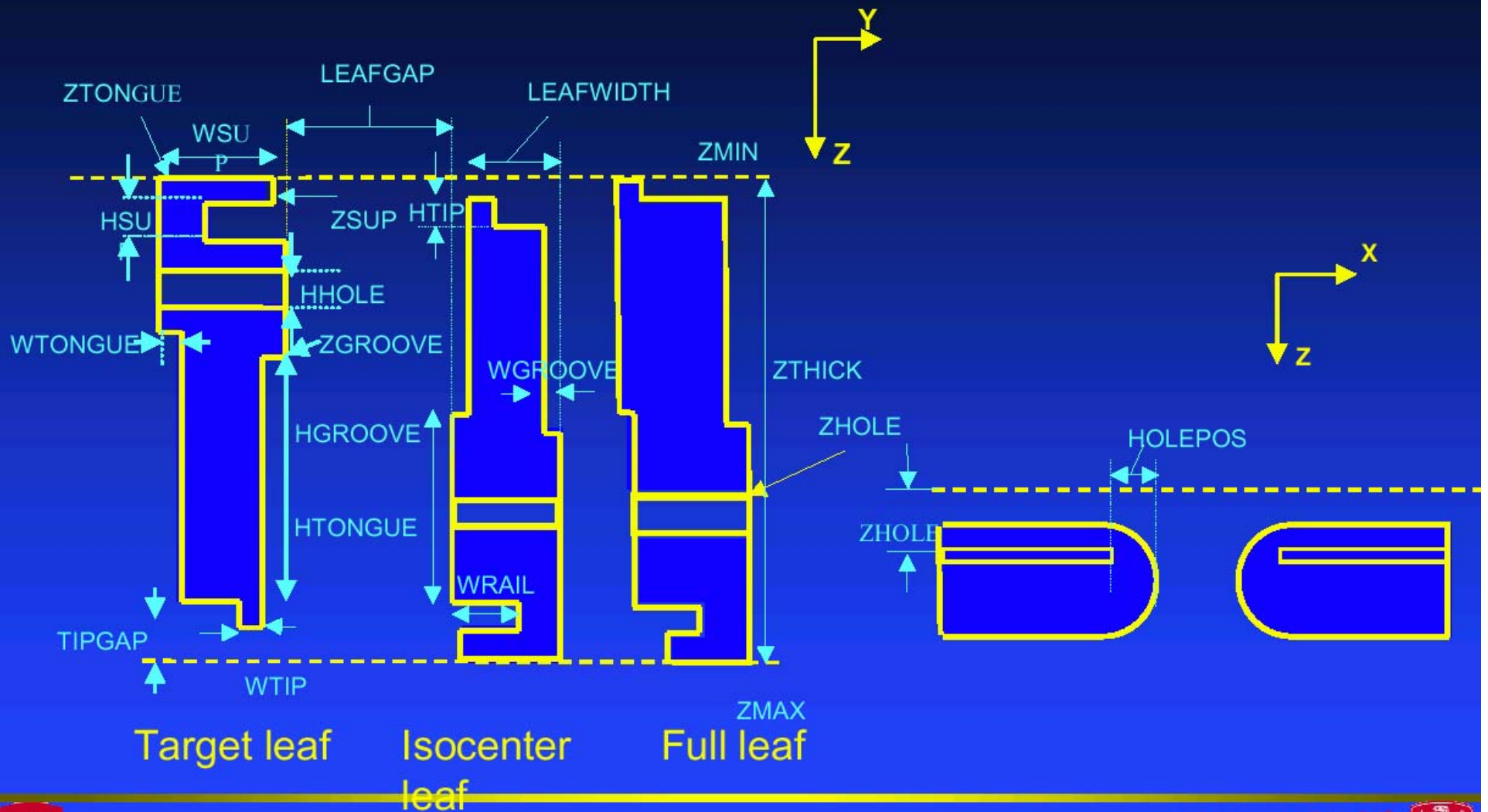


- leaf sides diverge with focus at 0 cm
- adjacent leaves are offset vertically
- leaf width = 0.23 cm

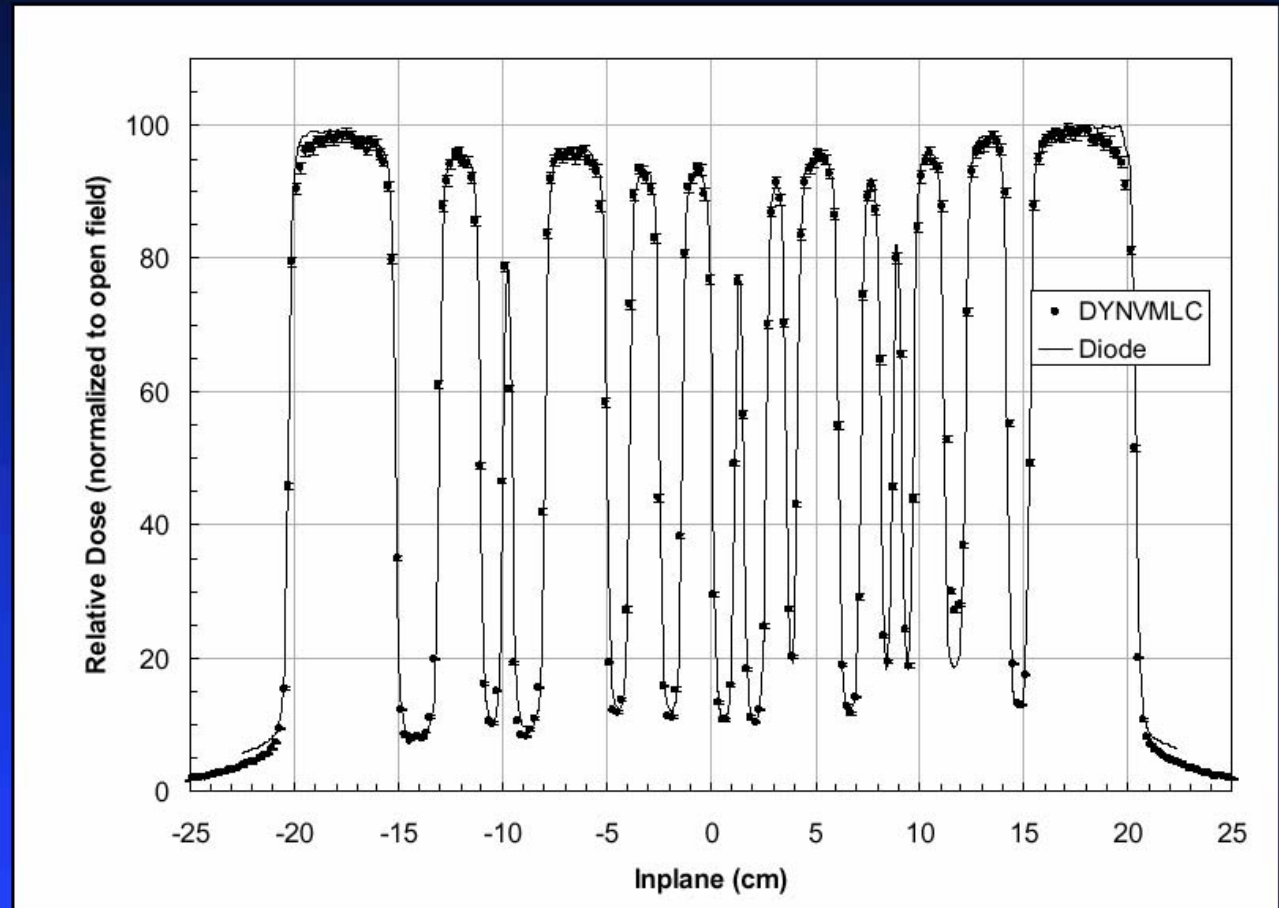
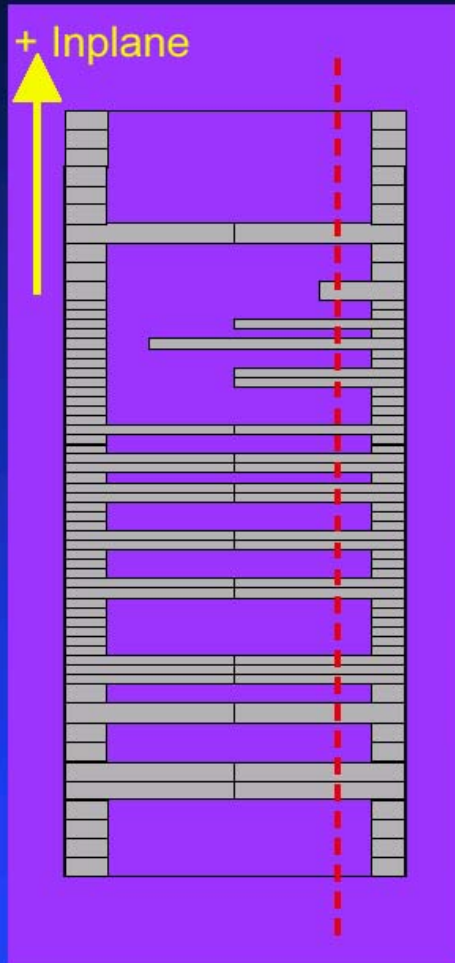




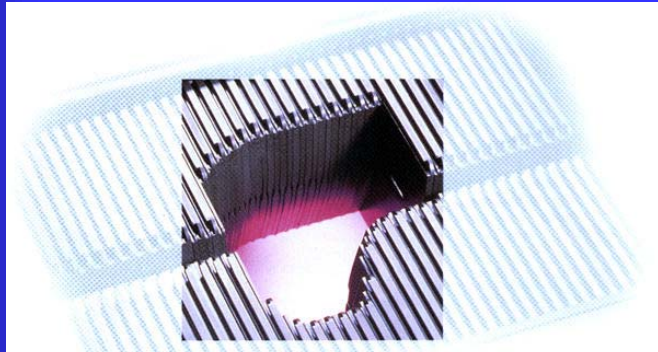
# DYNVMLC Component Module



# MLC bar pattern

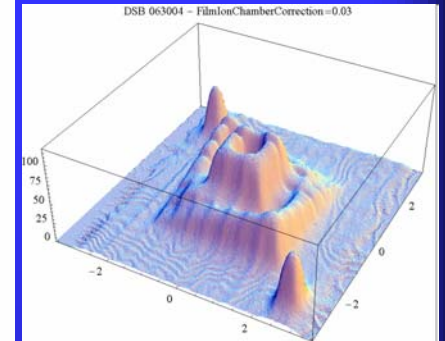
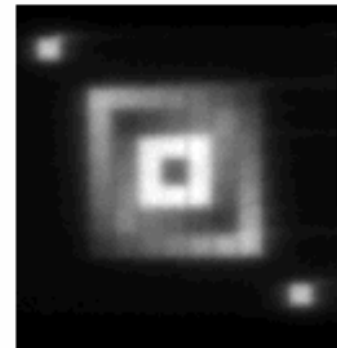
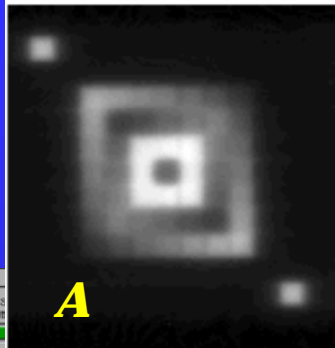


# MC calculated IMRT Patterns with MLC-120



measured

PEREGRINE



**A**

Study number: 1071 Treatment Unit: PG1.61 MLC120e - for commissioning training

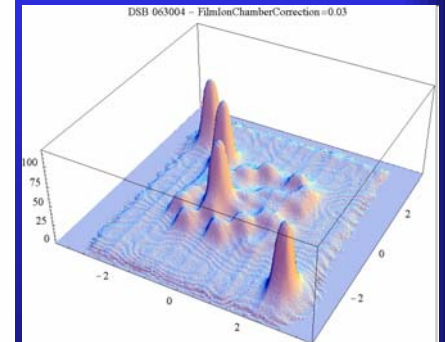
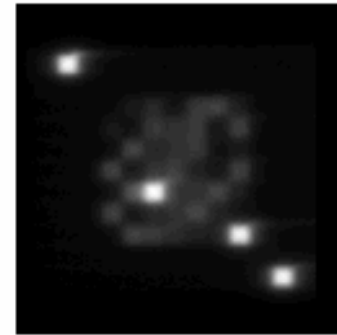
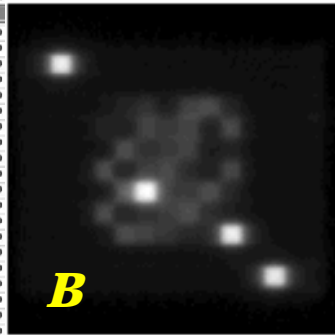
Planning System Calibration  
Calibration Factor: 1.000000

## CORVUS Beam Utilities

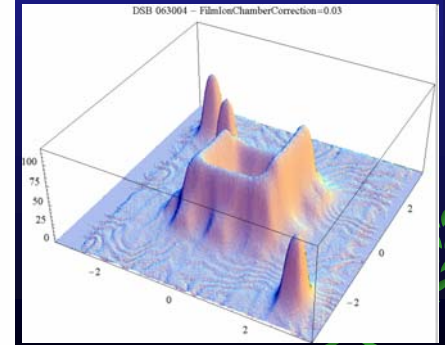
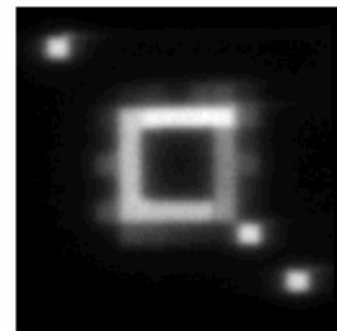
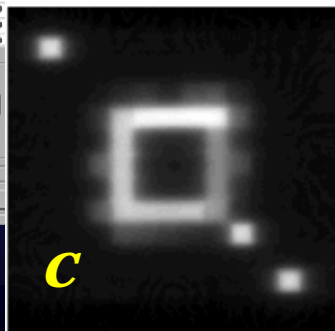
	X 21	X 22	X 23	X 24	X 25	X 26	X 27	X 28	X 29	X 30	X 31	X 32	X 33	X 34	X 35	X 36	X 37
V 42	0.0	0.0	0.0	0.0	0.0	0.0	0.0	0.0	0.0	0.0	0.0	0.0	0.0	0.0	0.0	0.0	0.0
V 41	0.0	0.0	0.0	0.0	0.0	0.0	0.0	0.0	0.0	0.0	0.0	0.0	0.0	0.0	0.0	0.0	0.0
V 40	0.0	0.0	0.0	0.0	0.0	0.0	0.0	0.0	0.0	0.0	0.0	0.0	0.0	0.0	0.0	0.0	0.0
V 39	0.0	0.0	0.0	0.0	0.0	0.0	0.0	0.0	0.0	0.0	0.0	0.0	0.0	0.0	0.0	0.0	0.0
V 38	0.0	0.0	0.0	0.0	0.0	0.0	0.0	0.0	0.0	0.0	0.0	0.0	0.0	0.0	0.0	0.0	0.0
V 37	0.0	0.0	0.0	0.0	0.0	0.0	0.0	0.0	0.0	0.0	0.0	0.0	0.0	0.0	0.0	0.0	0.0
V 36	0.0	0.0	0.0	0.0	0.0	0.0	0.0	0.0	0.0	0.0	0.0	0.0	0.0	0.0	0.0	0.0	0.0
V 35	0.0	0.0	0.0	0.0	0.0	100.0	0.0	0.0	0.0	0.0	0.0	0.0	0.0	0.0	0.0	0.0	0.0
V 34	0.0	0.0	0.0	0.0	0.0	0.0	0.0	0.0	0.0	0.0	0.0	0.0	0.0	0.0	0.0	0.0	0.0
V 33	0.0	0.0	0.0	0.0	0.0	0.0	80.0	70.0	60.0	50.0	40.0	30.0	20.0	0.0	0.0	0.0	0.0
V 32	0.0	0.0	0.0	0.0	0.0	0.0	70.0	10.0	20.0	30.0	40.0	50.0	30.0	0.0	0.0	0.0	0.0
V 31	0.0	0.0	0.0	0.0	0.0	0.0	60.0	20.0	100.0	100.0	100.0	80.0	40.0	0.0	0.0	0.0	0.0
V 30	0.0	0.0	0.0	0.0	0.0	0.0	50.0	30.0	100.0	100.0	100.0	30.0	50.0	0.0	0.0	0.0	0.0
V 29	0.0	0.0	0.0	0.0	0.0	0.0	40.0	40.0	100.0	100.0	100.0	20.0	60.0	0.0	0.0	0.0	0.0
V 28	0.0	0.0	0.0	0.0	0.0	0.0	30.0	50.0	40.0	30.0	20.0	10.0	70.0	0.0	0.0	0.0	0.0
V 27	0.0	0.0	0.0	0.0	0.0	0.0	20.0	30.0	40.0	50.0	60.0	70.0	80.0	0.0	0.0	0.0	0.0
V 26	0.0	0.0	0.0	0.0	0.0	0.0	0.0	0.0	0.0	0.0	0.0	0.0	0.0	0.0	0.0	0.0	0.0
V 25	0.0	0.0	0.0	0.0	0.0	0.0	0.0	0.0	0.0	0.0	0.0	0.0	0.0	0.0	0.0	100.0	0.0
V 24	0.0	0.0	0.0	0.0	0.0	0.0	0.0	0.0	0.0	0.0	0.0	0.0	0.0	0.0	0.0	0.0	0.0
V 23	0.0	0.0	0.0	0.0	0.0	0.0	0.0	0.0	0.0	0.0	0.0	0.0	0.0	0.0	0.0	0.0	0.0
V 22	0.0	0.0	0.0	0.0	0.0	0.0	0.0	0.0	0.0	0.0	0.0	0.0	0.0	0.0	0.0	0.0	0.0
V 21	0.0	0.0	0.0	0.0	0.0	0.0	0.0	0.0	0.0	0.0	0.0	0.0	0.0	0.0	0.0	0.0	0.0
V 20	0.0	0.0	0.0	0.0	0.0	0.0	0.0	0.0	0.0	0.0	0.0	0.0	0.0	0.0	0.0	0.0	0.0
V 19	0.0	0.0	0.0	0.0	0.0	0.0	0.0	0.0	0.0	0.0	0.0	0.0	0.0	0.0	0.0	0.0	0.0
V 18	0.0	0.0	0.0	0.0	0.0	0.0	0.0	0.0	0.0	0.0	0.0	0.0	0.0	0.0	0.0	0.0	0.0

Set Transmittance  
 Y (Inplane) Start: 1 End: 1  
 X (Crossplane) Start: 1 End: 1 Transmittance: 0.0 %  
 [Clear All] [Set All]

Revoke Treatment Unit



**B**



**C**

NOMOS/NAS Medical

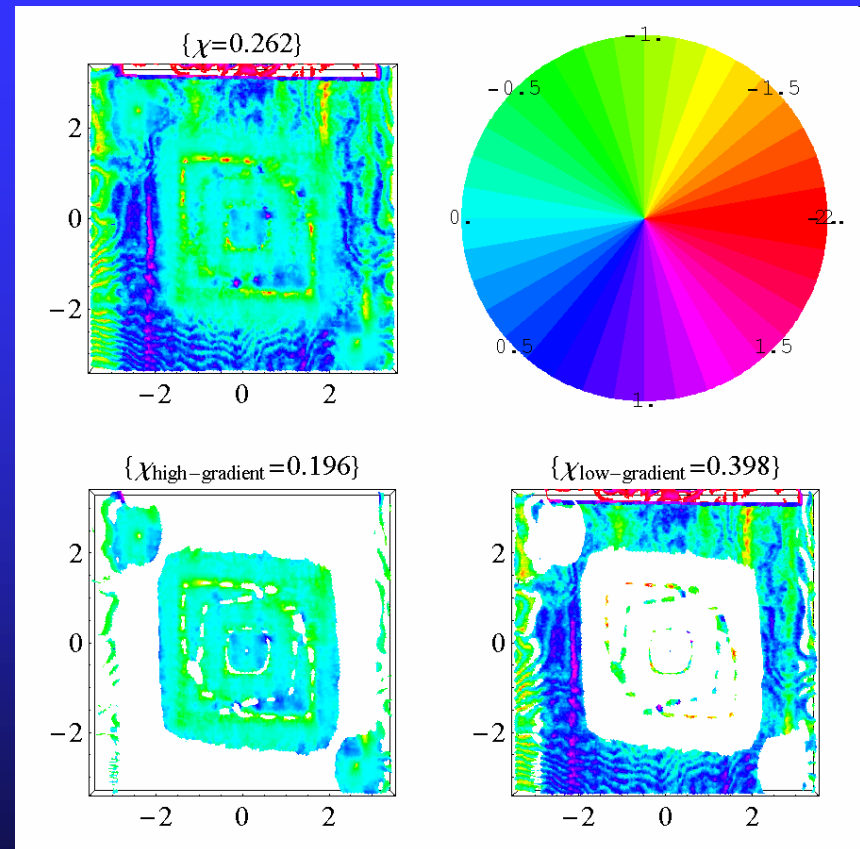
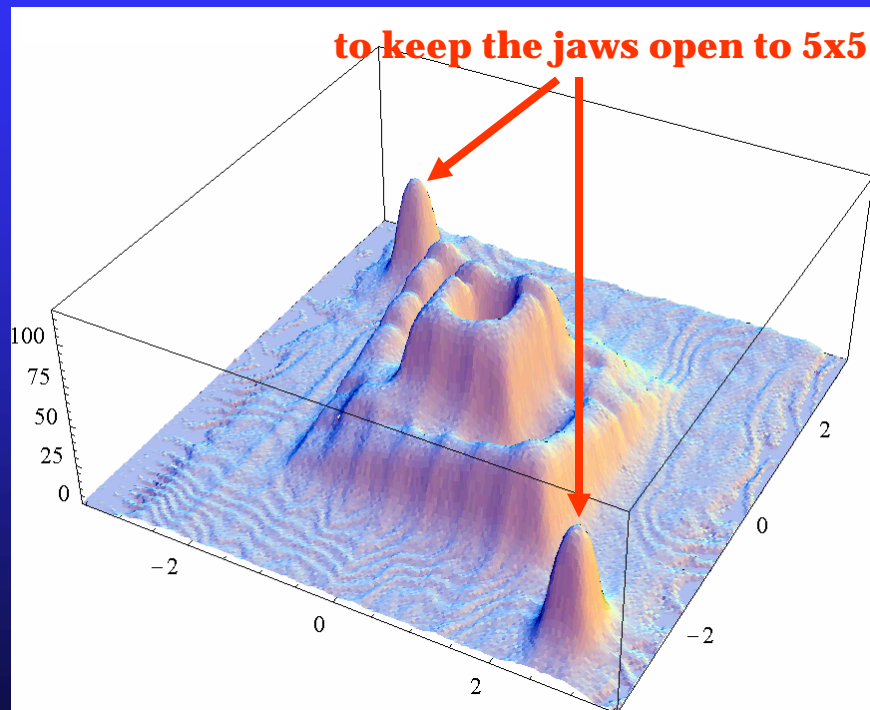
# 2-D Dose Analysis

CT Phantom: 512 x 512 x 83

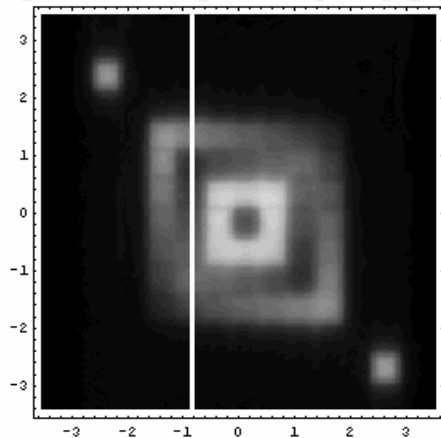
Dose Grid: 150 x 150 x 150 with 0.047 cm spacing. 1.5 % statistics

16 P-III 1 GHz

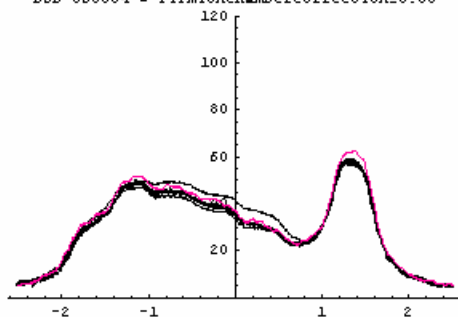
2050 MUs, 60 segments



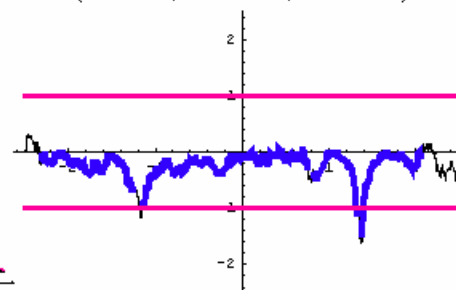
ABS\_NEW1.TIF, ComplexA\_highrescalc\_newRIT\_MI\_cf\_4\_resampled-calc.tif, 0.03)



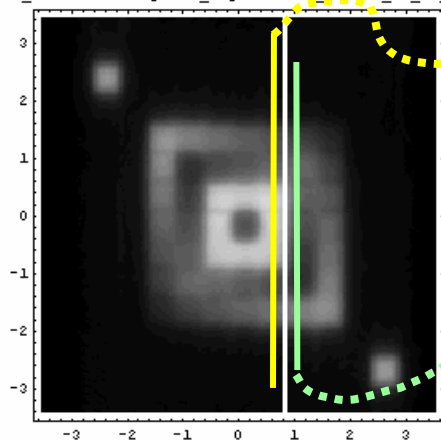
DSB 063004 - FilmIonChamberCorrection=0.03



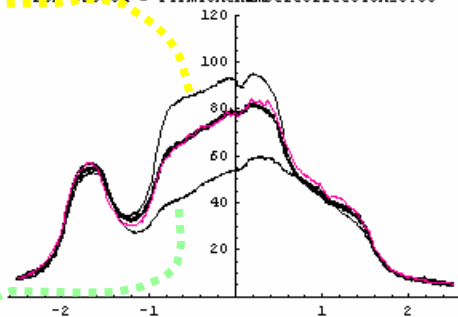
(Chi=0.245, ChiHG=0.239, ChiLG=0.272)



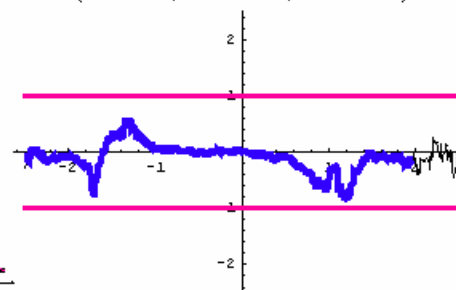
ABS\_NEW1.TIF, ComplexA\_highrescalc\_newRIT\_MI\_cf\_4\_resampled-calc.tif, 0.03)



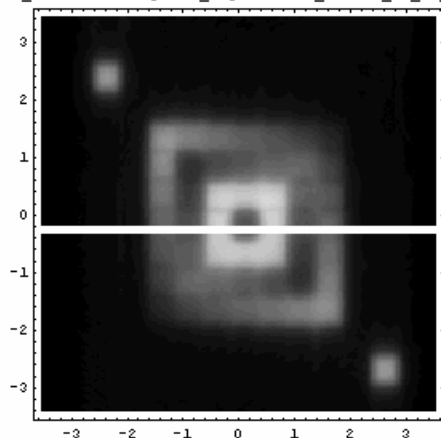
DSB 063004 - FilmIonChamberCorrection=0.03



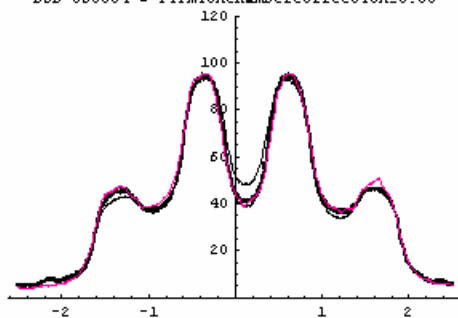
(Chi=0.175, ChiHG=0.181, ChiLG=0.139)



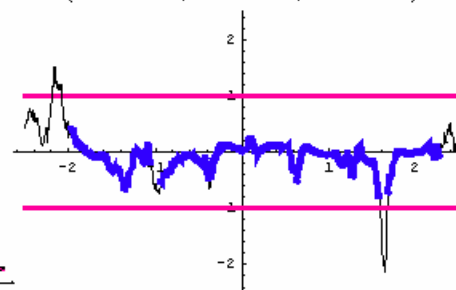
ABS\_NEW1.TIF, ComplexA\_highrescalc\_newRIT\_MI\_cf\_4\_resampled-calc.tif, 0.03)



DSB 063004 - FilmIonChamberCorrection=0.03



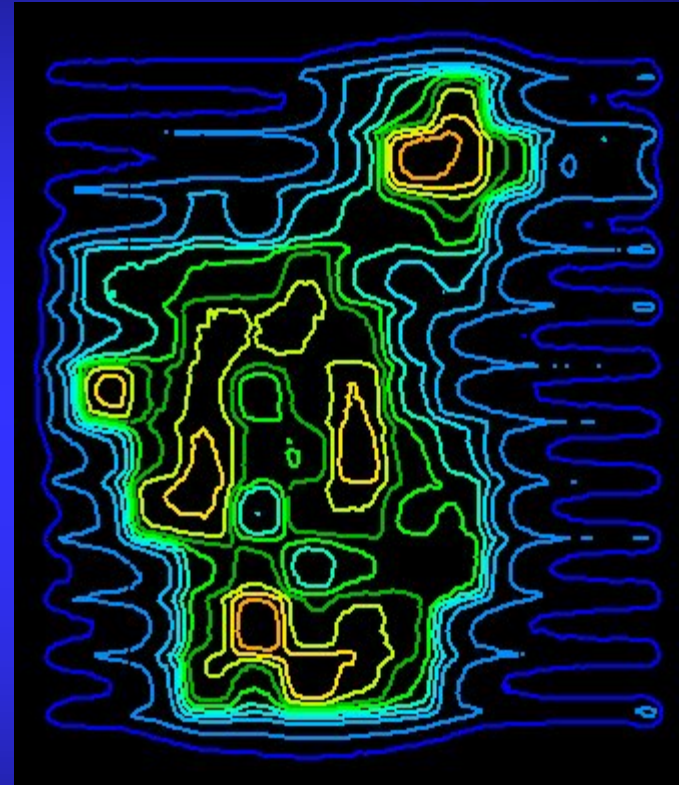
(Chi = 0.220, ChiHG=0.133, ChiLG=0.535)



# tongue-and-groove effect



Without



With

So much for "brute force" MC ...

Next, Charlie will talk about  
the design and utilization of  
MC Source Models ...

Thank you for your attention !

